

NN 08201

N: 575

C

COMPUTER SIMULATION OF
TRANSPORT PATTERNS OF
ASSOCIATING MACROMOLECULES

with special attention to

THE ELECTROPHORESIS OF
 α_{s1} - AND β -CASEIN

H. NIJHUIS

NN08201.575

BIBLIOTHEEK
DER
LANDBOUW HOGESCHOOL
WAGeningen

H. NIJHUIS

COMPUTER SIMULATION OF
TRANSPORT PATTERNS OF
ASSOCIATING MACROMOLECULES

with special attention to

THE ELECTROPHORESIS OF
 α_{s1} - AND β -CASEIN

PROEFSCHRIFT

TER VERKRIJGING VAN DE GRAAD
VAN DOCTOR IN DE LANDBOUW WETENSCHAPPEN,
OP GEZAG VAN DE RECTOR MAGNIFICUS,
PROF. DR. IR. H. A. LENIGER,
HOOGLERAAR IN DE TECHNOLOGIE,
IN HET OPENBAAR TE VERDEDIGEN OP WOENSDAG 16 JANUARI 1974
TE VIER UUR IN DE AULA VAN DE
LANDBOUWHOGESCHOOL TE WAGENINGEN

H. VEENMAN & ZONEN B.V. - WAGENINGEN - 1974

STELLINGEN

I

Het door CHOATE et al. waargenomen geheugen, dat de caseïnes bezitten, om micellen te vormen van een bepaalde grootte vindt een gerede verklaring in het voorkomen van complexen met verschillende stoechiometrie tussen de caseïne componenten.

W. L. CHOATE, F. A. HECKMAN en T. F. FORD, *J. Dairy Sci.*, **42** (1959) 761.

C. W. SLATTERY en R. EVARD, *Biochim. Biophys. Acta*, **317** (1973) 529.

dit proefschrift.

II

Bij het gebruik van gemethyleerde eiwitten als substraat voor het meten van proteolytische activiteiten moet bij de beoordeling van de resultaten rekening gehouden worden met de specificiteit van het betrokken enzym.

W. K. PAIK en S. KIM, *Biochemistry*, **11** (1972) 2589.

III

De wijze waarop JONES et al. de concentratie van cytochroom-B uit absorptie spectra bepalen kan tot zeer grote fouten aanleiding geven.

C. W. JONES, J. M. BRICE, V. WRIGHT en B. A. C. ACKRELL, *Febs Letters*, **29** (1973) 77.

C. W. JONES en E. R. REDFEARN, *Biochim. Biophys. Acta*, **143** (1967) 340.

IV

Er zijn bezwaren aan te voeren tegen de door NISHIYAMA en YAMADA voorgestelde massaspectrometrische fragmentatie van 3-aryl-5-chloormethyl-1,2,3-oxathiazolidine-2-oxides.

T. NISHIYAMA en F. YAMADA, *Bull. Chem. Soc. Japan*, **46** (1973) 2166.

V

De structuur die CRABBÉ en MISLOW voor het 7 β , 7' β -biërgostratriënol voorstellen op grond van de door hun gepresenteerde PMR-spectra is onjuist.

P. CRABBÉ en K. MISLOW, *Chem. Commun.*, **1968**, 657.

VI

De aanduiding „nieuw” voor de ruimtegroepebepaling van DRÄGER en GATTOW is overdreven.

M. DRÄGER en G. GATTOW, *Acta Cris.*, **B27** (1971) 1477.

VII

De door FOLTMANN voorgestelde genetische verklaring voor de (micro-)hetrogeniteit van rennine wordt op onvoldoende wijze door experimenten gesteund.

B. FOLTMANN, Compt. rend. trav. Lab. Carlsberg, 35 (8) (1966) 168.

N. ASATO en A. G. RAND, Biochem. J., 129 (1972) 841.

VIII

Vanuit didactisch oogpunt verdient het aanbeveling om in scheikunde-leerboeken voor de middelbare school stereoafbeeldingen op te nemen van de tetraëdrische omringing zoals die reeds in 1874 door VAN 'T HOFF is voorgesteld.

IX

Het is wenselijk, dat voor kinderen boven 14 jaar de leerplichtwet wordt vervangen door een leerrechtwet.

H. NDUIS

Wageningen, 16 januari 1973

VOORWOORD

Het verschijnen van dit proefschrift biedt mij een goede gelegenheid mijn dank te betuigen aan allen die tot mijn wetenschappelijke vorming hebben bijgedragen, in het bijzonder aan de Hoogleraren en Lectoren van de Faculteit voor Wiskunde en Natuurwetenschappen van de Universiteit van Amsterdam.

Tevens wil ik op deze plaats het Ministerie van Onderwijs en Wetenschappen bedanken dat mij materieel in staat heeft gesteld de universitaire studie te voltooien. Eveneens komt veel dank toe aan de Directie van het Nederlands Instituut voor Zuivelonderzoek en aan de Nederlandse Organisatie voor Zuiver-Wetenschappelijk Onderzoek, die het promotie-onderzoek hebben mogelijk gemaakt.

Hooggeleerde Veeger, hooggeschatte promotor, voor de mogelijkheid die U mij geboden hebt bij U te promoveren ben ik U zeer erkentelijk. Uw stimulerende belangstelling en de grote mate van vrijheid die ik bij het onderzoek mocht ondervinden heb ik altijd zeer gewaardeerd.

Zeergeleerde Payens, beste Theo, zeer veel dank ben ik aan jou verschuldigd voor de voortdurende aandacht die je aan dit proefschrift hebt besteed. Zonder jouw vele waardevolle suggesties en opbouwende kritiek zou dit proefschrift in zijn huidige vorm niet tot stand zijn gekomen.

Zeergeleerde Schmidt, zeergeleerde Vreeman, beste Daan en Henk, veel dank voor jullie adviezen en de nauwkeurige wijze waarop jullie het manuscript hebben doorgelezen.

Voorts wil ik mejuffrouw P. Both en de heer J. A. Brinkhuis bedanken, die door het verrichten van experimenteel werk een bijdrage hebben geleverd aan dit proefschrift.

Verder dank ik de heren H. J. van Brakel en J. Mondria voor het vervaardigen van de figuren en de heer G. H. Stel voor het zuiveren van de Engelse tekst.

Ten slotte wil ik de medewerkers van het Nederlands Instituut voor Zuivelonderzoek bedanken voor de ondervonden collegialiteit; deze heeft mij de vreugde in het werk vergroot en het leven, ook buiten het instituut, veraangenaamd.

CONTENTS

I INTRODUCTION	1
II FREE ELECTROPHORESIS OF COMPLEX FORMING α_{s1} - AND β -CASEIN	7
2.1. Introduction	7
2.2. Materials and methods	8
2.3. Results	9
2.4. Discussion	14
III COMPUTER SIMULATION OF ELECTROPHORETIC EXPERIMENTS	23
3.1. Introduction	23
3.2. Theory of the simulation method and discussion of the results	24
3.3. Alternative methods for the simulation of diffusional fluxes	31
IV A PROGRAM IN ALGOL FOR THE SIMULATION OF ELECTROPHORETIC REACTION BOUNDARIES OF INTERACTING BIOPOLYMERS	38
4.1. Construction of program	38
4.2. The computation parameters	42
4.3. The program lists	43
SUMMARY	53
SAMENVATTING	54
REFERENCES	55

I INTRODUCTION

The study of biopolymer interactions – e.g. polymerization and complex formation of proteins and nucleic acids and to a less extent of polysaccharides – has received considerable interest during the last few decades (REITHEL, 1963; NICHOL et al., 1964; SUND and WEBER, 1966; KLOTZ, 1967). This is due, no doubt, to the central role of such interactions in a number of widely divergent biological phenomena, such as the complex formation between a proteolytic enzyme and its substrate, an antigen and an antibody and the association between RNA and coat protein in virus particles.

The quantitative evaluation of the thermodynamic parameters involved in these associations has also reached a very satisfactory level.

Among the methods by which the interactions of biopolymers can be studied two different approaches may be distinguished. First, those measuring techniques in which thermodynamic equilibrium is maintained such as osmometry, light scattering and sedimentation equilibrium. Second, transport methods such as free electrophoresis, sedimentation velocity and gel chromatography in which the equilibrium between the reactants is continuously perturbed by application of an external potential field. Both kinds of methods may complement each other. Typical examples are the studies of the tetramerization of β -lactoglobulin (TOWNEND et al., 1960A, 1960B; TOWNEND and TIMASHEFF, 1960; TIMASHEFF and TOWNEND, 1961), the polymerization of chymotrypsin (RAO and KEGELES, 1958) and the self-association of α_{s1} -casein (PAYENS and SCHMIDT, 1966; SCHMIDT, 1970).

With the equilibrium techniques mentioned above apparent molecular weights are obtained as a function of concentration. For example with light scattering and sedimentation equilibrium in the ultracentrifuge an apparent molecular weight is obtained (TANFORD, 1967; FUJITA, 1962) which is connected to the weight average molecular weight,

$$\bar{M}_w = \frac{\sum_i c_i M_i}{\sum_i c_i} \text{ by}$$

$$1/M_a = 1/\bar{M}_w + 2\bar{B}c + O(c^2) \dots \quad (1.1)$$

The mean second virial coefficient, \bar{B} , is obtained by averaging the interaction parameters B_{ij} of the species i and j which are connected to the activity coefficients f_i by the following equation (FUJITA, 1962):

$$\ln f_i = M_i \sum_j B_{ij} c_j + O(c^2) \quad (1.2)$$

STEINER (1954, 1970A, 1970B) has developed graphical procedures to obtain the association constants from the concentration dependence of the apparent

molecular weight of polymerizing and complex forming proteins. A thorough discussion of the difficulties involved in the separation of the contributions of non-ideality (excluded volume effects) and association to the apparent molecular weights of polymerizing systems has been given by SCHMIDT and PAYENS (1972).

Independent information about the degree of polymerization of self-associating systems and of the association constants involved can also be obtained from the anomalies of the boundaries observed in transport experiments such as electrophoresis and ultracentrifugation (GILBERT, 1958; GILBERT and JENKINS, 1959). An additional advantage of this approach is that it may directly be concluded whether the self-association of the system under investigation is of the open or the discrete type. An open association is defined as one in which the polymers of a number of consecutive association steps are present simultaneously, whereas in discrete polymerization only one degree of polymerization is favoured.

GILBERT (1958) and GILBERT and JENKINS (1959) have given analytical solutions of the conservation-of-mass equation of relatively simple associating systems ($nA \rightleftharpoons A_n$ and $A + B \rightleftharpoons AB$) during sedimentation or electrophoresis. In their theory these authors neglected the effect of diffusion and non-ideality on the spreading of the boundaries and the re-adjustment of the chemical equilibrium was assumed to be rapid as compared with the difference in migration of the various components. The first approximation actually means that the migration pattern is extrapolated to infinite time, since the spreading of a boundary due to diffusion is proportional to the square root of the time, whereas the spreading due to differential migration of the components is proportional to the time itself. The second approximation comes to accepting the velocities to be independent of concentration and neglecting activity coefficients in the definition of the equilibrium constants.

Some important conclusions from GILBERT's theory are the following.

1. In the case of dimerization sedimentation in the ultracentrifuge yields an asymmetric peak with a trailing edge. The same conclusions hold true for the trailing boundary in gel filtration since the migration behaviour in both cases is similar. The ascending electrophoretic boundary and the leading boundary in gel filtration, however, are found to be hypersharp and to move with weight-average velocities (GILBERT, 1958; ACKERS, 1967).
2. In the case of discrete polymerization of the type $nA \rightleftharpoons A_n$ with $n > 2$ sedimentation will result in a bimodal peak. The degree of polymerization and the association constants can be obtained from the velocities of the maxima and minimum in the concentration gradient curves and the area distribution over the peaks. The same results are obtained from the trailing boundary in gel filtration (WINZOR and SCHERAGA, 1963). The leading boundaries in gel filtration and electrophoresis again will be hypersharp.
3. In the case of an open association similar pictures are obtained as with dimerization. These cases can be distinguished from each other by analysis of the velocities of the peaks.

4. In the case of a complex forming system $A + B \rightleftharpoons AB$ special attention should be given to the velocity of the complex as compared to that of the components A and B . In sedimentation and gel filtration the velocity of the complex normally will be larger than that of each constituent (SCHACHMAN, 1959; ACKERS, 1970), whereas in electrophoresis the complex usually is observed to move with an intermediate velocity (GILBERT and JENKINS, 1959). As a result in electrophoresis the leading ascending and the trailing descending peaks move with the mobilities of the pure components A and B respectively (cf. Figure 1.1). The other peaks have intermediate velocities and therefore can neither be identified with component A nor with component B . Sometimes these so-called reaction boundaries are found to be bimodal, depending on the association constants and initial concentrations. An important result of the GILBERT-JENKINS theory is that the ascending and descending patterns in electrophoresis are highly non-enantiographic as a consequence of complex formation. As stated above this non-enantiography may even result in a different number of peaks on both sides of the electrophoretic U-tube. It should be remembered that normally in free electrophoresis non-enantiography also appears as a result of the conductivity changes along the electrophoretic channel. As is well known this effect arises as a consequence of the constancy of the Kohlrausch regulating function (LONGWORTH, 1959) and is manifested by the appearance of the δ - and ϵ -boundaries (see Figure 1.1) and conductivity changes along the electrophoretic channel. In contrast to the non-enantiography due to complex formation, however, the latter effect will never result in a different number of moving boundaries on both sides of the electrophoretic channel and can be suppressed by diluting the protein solution with respect to the electrophoresis buffer.

Complex forming systems of the type, $A + B \rightleftharpoons AB$, may also be analysed using the moving boundary theory developed by LONGWORTH (1959) for free electrophoresis (see also NICHOL and WINZOR, 1962; SCHACHMAN, 1959). Following LONGWORTH, the electrophoretic channel is divided in phases with constant concentrations and velocities, which are termed a, b, c, d etc. on the ascending side and α, β, γ etc. on the descending side (cf. Figure 1.1) where a and α refer both to the undisturbed protein solution. For the simple complex forming system referred to above, LONGWORTH derived the following equations:

$$C_B^\beta = \bar{C}_B^\alpha \frac{U_A^\alpha - U_B^\alpha}{U_A^\alpha - U_B^\beta} \quad (1.3)$$

and

$$C_A^\alpha = (\bar{C}_A^\alpha + C_B^\beta - \bar{C}_B^\alpha) \frac{U_A^\alpha - U_B^\alpha}{U_A^\alpha - U_B^\beta} \quad (1.4)$$

In these equations C_B^β refers to the mass concentration of component B in the β -phase (cf. Figure 1.1). Further \bar{C}_A^α and \bar{C}_B^α are the constituent concentrations of A and B in the α -phase which are defined as

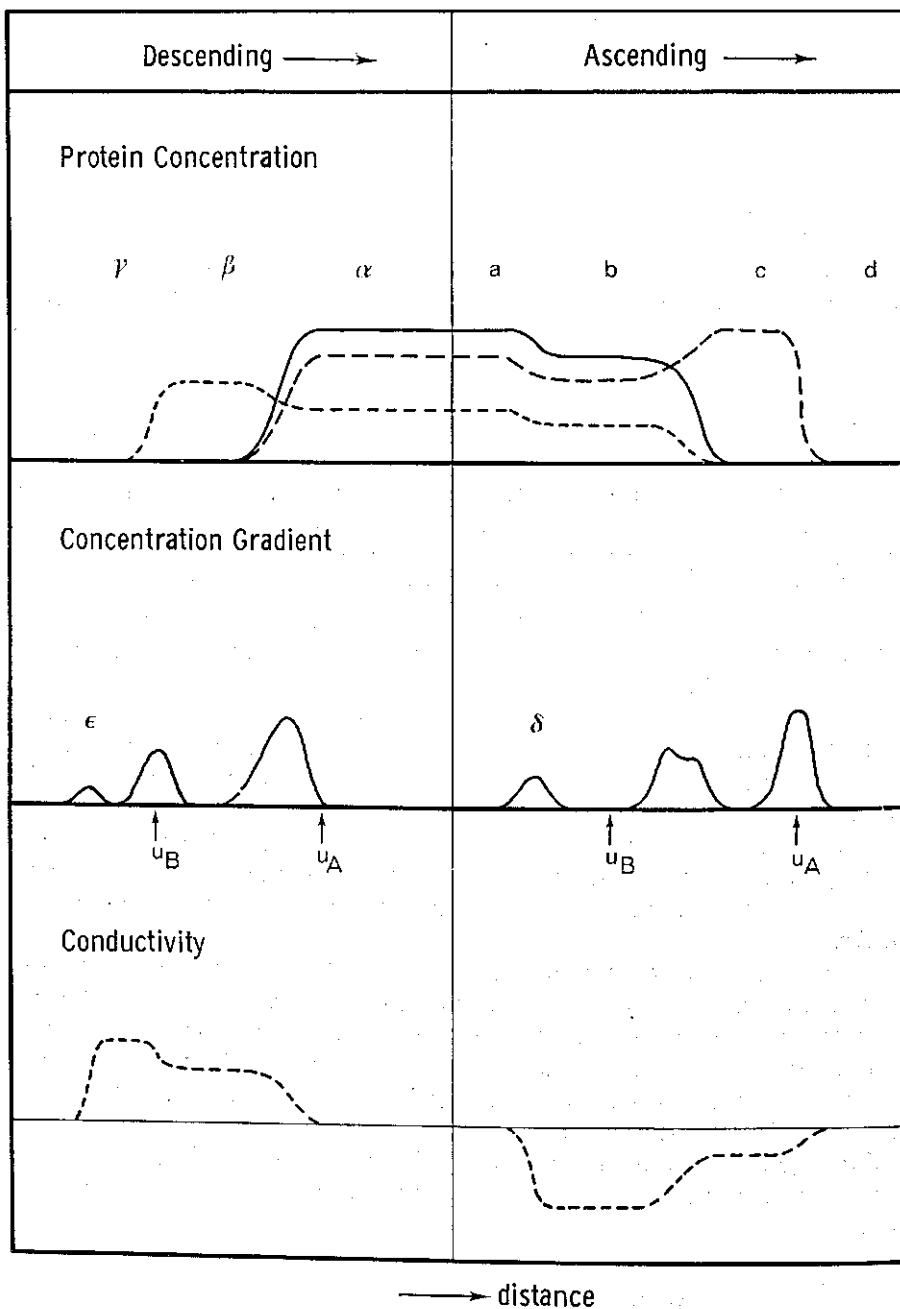


FIG. 1.1 Schematic picture of moving boundary electrophoresis of the reacting system $A + B \rightleftharpoons AB$,

a. Concentration distribution after transport; a, b, c, d, α , β and γ indicate phases of constant concentrations and mobilities.

b. Schlieren pattern of the system after transport; ϵ and δ are the stationary boundaries caused by the constancy of the Kohlrausch regulating function.

c. Conductivity changes along the electrophoretic channel:

— initial conductivity level;

--- changes brought about by transport.

$$\left. \begin{aligned} \bar{C}_A^\alpha &= C_A^\alpha + C_{AB}^\alpha \\ \bar{C}_B^\alpha &= C_B^\alpha + C_{AB}^\alpha \end{aligned} \right\} \quad (1.5)$$

\bar{U}_A^α and \bar{U}_B^α are the constituent velocities of *A* and *B* in the α -phase and were defined by LONGSWORTH as

$$\left. \begin{aligned} \bar{U}_A &= (U_A C_A + U_{AB} C_{AB}) / \bar{C}_A \\ \bar{U}_B &= (U_B C_B + U_{AB} C_{AB}) / \bar{C}_B \end{aligned} \right\} \quad (1.6)$$

\bar{U}_A^α and \bar{U}_B^β are measured from the volumes swept through by the $\alpha\beta$ - and bc -boundaries respectively (LONGSWORTH, 1959). From Equation 1.4 and the known constituent concentrations of *A* and *B* the equilibrium constants may be calculated. In systems of higher stoichiometry Equation 1.4 can no longer be applied. It is still possible, however, to obtain useful information concerning the stoichiometry of the complexes by application of Equation 1.3 as will be demonstrated in Chapter 2.

This thesis will deal specifically with the electrophoretic analysis of the complex formation between α_{s1} - and β -casein, two major proteins from cow's milk (JENNESS, 1970).

The caseins occur in milk (JENNESS, 1970) as nearly spherical colloidal particles with diameters up to 300 nm: the casein micelle. The micelle also contains approximately 5% of inorganic constituents of which calcium and phosphate are the most important (WAUGH, 1971). The protein part of the casein micelle is composed of three major components: α_{s1} - and β -casein, mentioned already above and κ -casein. Casein micelles behave more or less like hydrophobic colloids and already LINDERSTRÖM LANG (1929) hypothesized the existence of a protective component, stabilizing the micelles against flocculation by calcium ions. In 1956 WAUGH and VON HIPPEL rediscovered this stabilizing component and called it κ -casein.

The stabilizing properties are completely destroyed after the action of the enzyme rennin, which results in the splitting-off of a polypeptide from κ -casein with a length of approximately one third of the whole polypeptide chain (MACKINLAY and WAKE, 1971). The remaining part of the κ -casein, which is called para- κ -casein no longer stabilizes the casein micelle and as a consequence flocculation occurs. As is well known this process forms the basis of the cheese manufacturing.

From electronmicroscopy it has become clear that casein micelles are composed of a large number of small particles, called the submicelles (SCHMIDT and BUCHHEIM, 1970). Dialysis experiments suggest that these submicelles contain mere casein. The casein micelles are therefore considered to be conglomerates of submicelles cemented together by inorganic ions, notably Ca^{++} . The hypothesis according to which it is supposed that the submicelles are the

fundamental parts of the casein micelles is supported by recent work concerning the size distribution of the casein micelles (SCHMIDT et al., 1973), by electronmicroscopical analysis of the calcium distribution in casein micelles (KNOOP et al., 1973) and by electronmicroscopic studies concerning the biosynthesis of the micelles in the golgi vesicles in the mammary gland (BUCHHEIM and WELSCH, 1973).

The precise structure of the casein micelles and in particular the structure and composition of the submicelles is not yet known. Clearly, interactions between the casein components will be of primary importance in this respect. It is obvious that caseins, being proteins with an open, more or less randomly coiled like structure (HERSKOVITS, 1966) and containing a more than average proportion of amino acids with non-polar side chains (WAUGH, 1954) have numerous possibilities for interaction through hydrophobic bonding. This has been amply verified in a number of polymerization studies during the last decade.

The self-association of α_{s1} - and β -casein has been studied in particular (PAYENS and VAN MARKWIJK, 1963; PAYENS et al., 1969; SCHMIDT, 1969, 1970; SCHMIDT and PAYENS, 1972). It was found that α_{s1} -casein associates mainly by hydrophobic interaction and to a less extent by hydrogen bonding (SCHMIDT, 1969; SCHMIDT and PAYENS, 1972) whereas the association of β -casein is probably entirely due to hydrophobic bonding (PAYENS et al., 1969). Also κ -casein associates strongly (SWAISGOOD et al, 1964), but a full description of this association has not yet been given.

From the non-specificity of the bonds formed during self-association of α_{s1} - and β -casein, it might be anticipated that the same type of bond will be formed with the complex formation between these casein components. Complex formation in total casein has already been observed by KREJCI et al. (1941), KREJCI (1942) and WARNER (1944) also applying the technique of free electrophoresis. The quantitative description of such complex formation is greatly complicated, however, by the self-association of the components. This results in the simultaneous occurrence of more than one association equilibrium which cannot be analysed with the simple theory of GILBERT and JENKINS, referred to above. The numerical solution of this problem in the case of the simultaneous association equilibria in the system α_{s1} - and β -casein will be given in the next chapter of this thesis.

From the foregoing it will be clear that the study of the interactions between the different casein components will be of paramount importance for our understanding of the energetics of the casein micelles in milk and of their behaviour in a number of technological processes such as pasteurization, sterilization, concentration and homogenization. Also gelation of dairy products after UHTST heat treatment and the curdling of milk, will partly be influenced by the interaction between the caseins.

It should be emphasized that the analysis of reaction boundaries by the methods developed in this thesis is certainly not limited to the complex formation of the caseins. It may also be applied with equal success to interactions between other proteins or macromolecules of which examples have already been mentioned at the beginning of this chapter.

II FREE ELECTROPHORESIS OF COMPLEX FORMING α_1 - AND β -CASEIN

2.1. INTRODUCTION

The study of interacting biopolymers by such transport methods as sedimentation, electrophoresis and gel filtration has received considerable impetus over the last decades (LONGSWORTH, 1959; NICHOL et al., 1964; ACKERS, 1970; CANN and GOAD, 1970). The relevancy of such studies is indicated by a number of biochemical phenomena in which complex formation plays a central role. As early as 1942, LONGSWORTH and MACINNES investigated the complex formation between a protein (ovomucoid) and nucleic acid (yeast RNA) by free electrophoresis and formulated the anomalies to be expected in the electrophoretic patterns. Further examples are the study of the enzyme/substrate complex between pepsin and bovine serum albumin by CANN and KLAPPER (1961) and that of antigen/antibody interaction by SINGER and CAMPBELL (1955). The complex formation between bovine plasma albumin and charged dextran derivatives was studied by THOMPSON and MACKERNAN (1961).

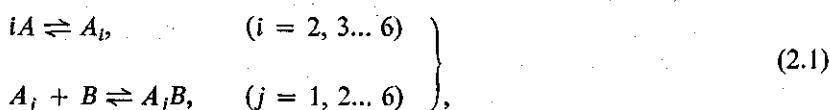
In such studies the advantage of free electrophoresis and gel filtration over sedimentation lies in the fact that with the former techniques two moving boundaries are observed, whereas during ultracentrifugation only one. In electrophoresis the non-enantiography of rising and descending patterns yields additional information which is lacking in the sedimentation experiment and which often facilitates diagnosis.

Rapid progress in our understanding of the electrophoretic behaviour of interacting proteins is due to GILBERT and JENKINS (1959), who solved the conservation-of-mass equation for the equilibrium system $A + B \rightleftharpoons AB$. The GILBERT theory accepts fast re-adjustment of the equilibrium upon changes in concentration brought about by transport and neglects the influence of diffusion on the spreading of the boundaries. Another limitation of the theory is that the velocities are assumed to be constant, which is neither true in sedimentation (FUJITA, 1962; PAYENS and SCHMIDT, 1966) nor in electrophoresis (LONGSWORTH, 1959). Despite these restrictions, the GILBERT theory explains quite satisfactorily the anomalies observed during electrophoresis or sedimentation of complex forming biopolymers. Notably GILBERT and JENKINS (1959) were able to account for the occurrence of a different number of moving peaks on both sides of the electrophoretic channel and for their abnormal mobilities and percentages. The close resemblance of a number of experimental electrophoretic patterns (NICHOL et al., 1964; LONGSWORTH and MACINNES, 1942; CANN and KLAPPER, 1961; SINGER and CAMPBELL, 1955; THOMPSON and MACKERNAN, 1961) to those computed by GILBERT and JENKINS suggests that as a rule rapid re-equilibration occurs during electrophoresis of interacting biopolymers. As regards the diffusion, its influence on the spreading of the moving

boundary may often be neglected in prolonged experiments, as shown by BALDWIN (1957) and by GILBERT and JENKINS (1959). However, there always remains the possibility that small peaks or shoulders are obscured by the blurring effect of diffusion. This suspicion has prompted a number of authors (CANN and GOAD, 1970, 1965A, 1965B; BETHUNE, 1970; COX, 1965A, 1965B, 1967, 1971A, 1971B) to solve the complete conservation-of-mass equation by various simulation methods. The simulation technique applied in the present study is described in the next chapters.

This chapter deals especially with the complex formation between α_{s1} - and β -casein, two major proteins from milk, the self-association behaviour of which is well known (SCHMIDT and PAYENS, 1972; SCHMIDT, 1970; PAYENS and VAN MARKWIJK, 1963). Under the experimental conditions of free electrophoresis, i.e. 2°C., pH 6.5 and an ionic strength of 0.1, β -casein is completely depolymerized (PAYENS and VAN MARKWIJK, 1963), whereas α_{s1} -casein undergoes a number of consecutive association steps, the association constants of which have been firmly established by SCHMIDT (1970). The study of α_{s1} - β complex formation is of paramount importance to our understanding of the energetics of casein micelle formation in milk (PAYENS, 1966; WAUGH, 1971).

The results of the present investigation suggest that multiple association equilibria occur, which can be represented by



in which A and B stand for α_{s1} - and β -casein respectively.

Preliminary reports of this investigation were published earlier (PAYENS, 1968; NIJHUIS and PAYENS, 1972).

The pertinency of this study is by no means restricted to the field of casein chemistry. It could well stand as a model for all those complex formations in which one of the components is subjected to self-association. The interaction between virus coat protein and RNA is an outstanding example of such a system (DURHAM et al., 1971; BUTLER and KLUG, 1972).

2.2. MATERIALS AND METHODS

Alpha_{s1}-casein was isolated from bulk milk by the method of SCHMIDT and PAYENS (1963), whereas β -casein was prepared in the manner described by PAYENS and VAN MARKWIJK (1963).

For electrophoresis the protein solutions were dialysed exhaustively against the appropriate buffer. The buffer of the last dialysis step was also used for the electrophoretic experiment. In those experiments where the salt anomaly had to be suppressed, the solution was enriched with protein and diluted after completion of dialysis (WIEDEMANN, 1947).

Sedimentation runs were performed in the Phywe air-driven ultracentrifuge under conditions comparable to those applied during electrophoresis.

Sedimentation coefficients, electrophoretic mobilities and peak areas were determined from enlarged tracings by routine measurements (LONGSWORTH, 1959; ELIAS, 1964).

The computations simulating the electrophoretic transport were performed with the university CDC-3200 digital computer. The source program was written in ALGOL-60. Details concerning the simulation procedure are given in Chapter 3 and 4.

2.3. RESULTS

Typical electrophoretic patterns of mixed solutions of α_{s1} - and β -casein in two types of buffer are shown in Figure 2.1. Peak mobilities and percentages from these and other experiments have been collected in Table 2.1. The fast formation of complexes between α_{s1} - and β -casein is clearly indicated by the different number of moving peaks on the ascending and descending sides (GILBERT and JENKINS, 1959). The mobilities of the trailing ascending and leading descending peaks, which are intermediate between those of pure α_{s1} - and β -casein and the abnormal distribution of the protein over the different peaks also afford convincing evidence of complex formation (LONGSWORTH, 1959; GILBERT and JENKINS, 1959). As is shown by comparison of the patterns of Figure 2.1a and 2.1c or 2.1b and 2.1d and the data in Table 2.1, buffer composition does not influence the general appearance of the electrophoretic patterns. Protein-buffer interactions seem therefore to be of no importance to the explanation of the anomalies observed (CANN and GOAD, 1970). Table 2.1 actually suggests that the mobilities of the complexes formed are intermediate between those of pure α_{s1} - and β -casein (GILBERT and JENKINS, 1959)*.

The fast re-equilibration of the complex formation during the electrophoretic transport was further checked by comparing experiments at different field strengths. Figures 2.2a and 2.2b and the data in Table 2.1 demonstrate that indeed variation of the field does not affect the mobilities and percentages of the electrophoretic patterns, confirming rapid re-equilibration. The electrophoretic patterns in Figures 2.1 and 2.2 show well-developed δ - and ε -boundaries. As is well known (LONGSWORTH, 1959), these boundaries are due to the constancy of the KOHLRAUSCH regulating function, as a result of which considerable conductivity changes may occur along the electrophoretic channel. A related consequence is – as was already pointed out by SVENSSON (1946) – that the fastest peaks are always enlarged at the cost of the slower ones.

The dilution factor, ρ , occurring at the δ -boundaries in Figures 2.1 and 2.2, was estimated in two independent ways.

* The relatively high mobilities observed with the 70/30 mixture in phosphate buffer probably should be explained by leakage during the electrophoretic experiment.

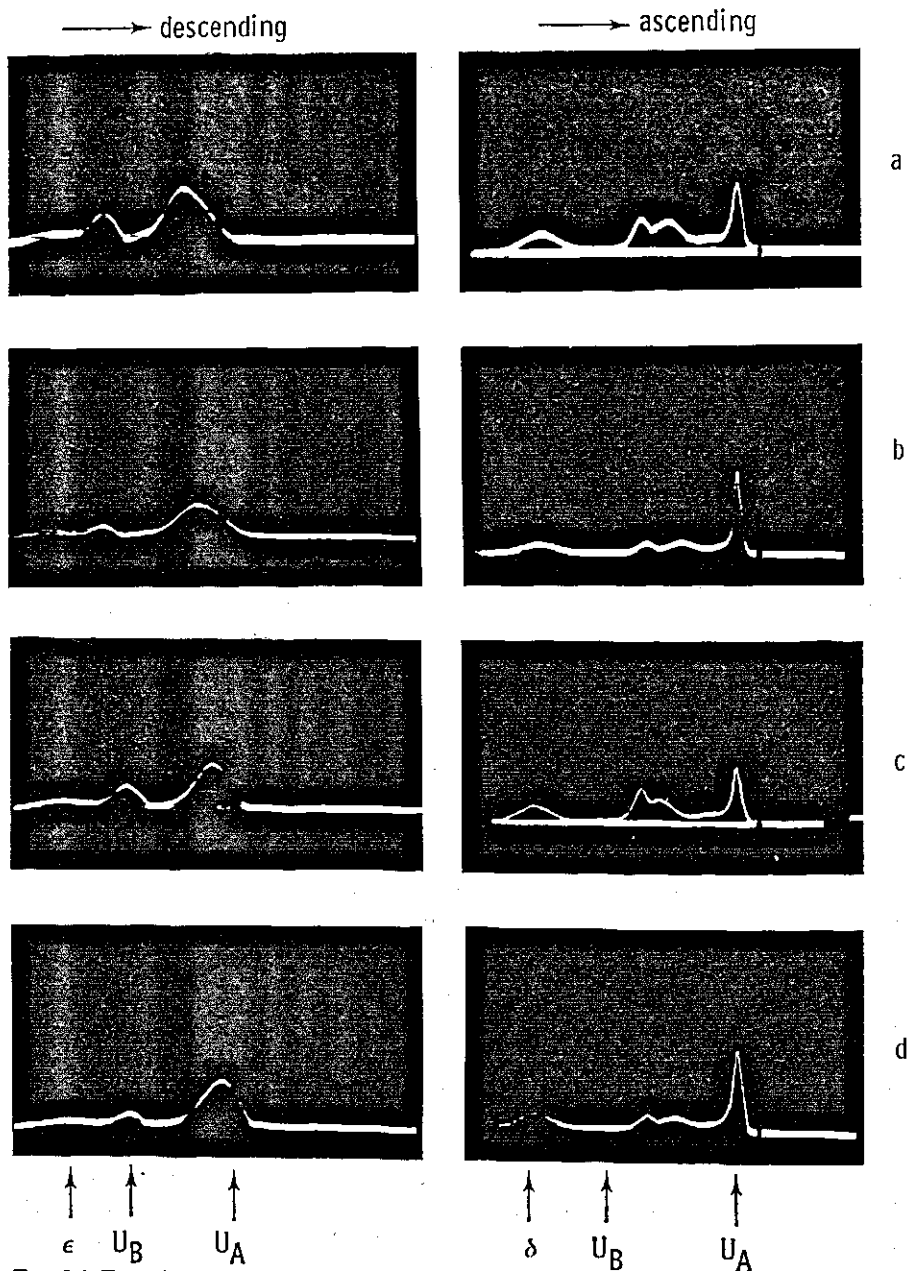


FIG. 2.1 Free electrophoresis of mixtures of α_{s1} - and β -casein at a total protein concentration of 1.20 g/dl. Experimental conditions: pH 6.6, 0.1 ionic strength and 2°C. Pictures taken after 4800 s.

Mixing ratio:

- a. $\alpha_{s1}/\beta = 50/50$; barbiturate buffer;
- b. $\alpha_{s1}/\beta = 70/30$; barbiturate buffer;
- c. $\alpha_{s1}/\beta = 50/50$; phosphate buffer;
- d. $\alpha_{s1}/\beta = 70/30$; phosphate buffer.

TABLE 2.1 Electrophoresis of α_{s1} - and β -casein at pH 6.6 and 0.1 ionic strength; field strength 3.05 (V/cm).

Mixing Ratio α_{s1}/β	Protein Concentration (g/dl)	Buffer	Ascending		Descending	
			Mobilities (10^{-5} cm ² /V s)	% ¹	Mobilities (10^{-5} cm ² /V s)	%
Pure α_{s1}	0.77	barbiturate	8.4		6.8	
70/30	1.20	barbiturate	8.4	52	6.3	86
70/30	1.20	phosphate	8.9	54	7.2	86
50/50	1.20	barbiturate	8.2	31	5.8	74
50/50	1.20	phosphate	8.3	32	6.5	70
50/50 ²	1.20	barbiturate	8.0	35	6.1	67
Pure β	0.80	barbiturate		3.2	2.7	33

¹ Total area under bimodal peak.

² Field strength 1.00 (V/cm).

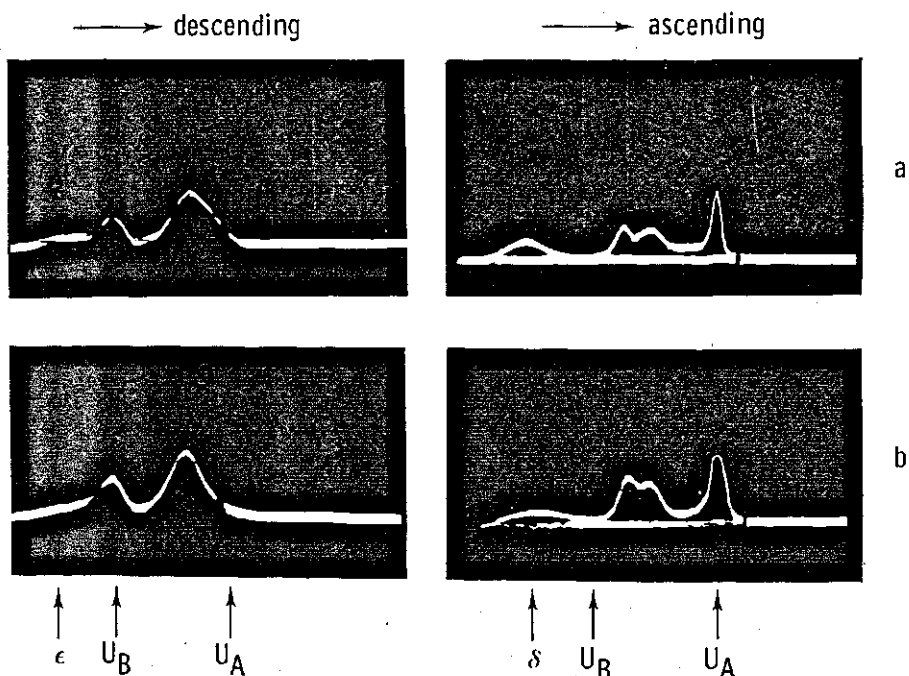


FIG. 2.2 Free electrophoresis of a 1:1 mixture of α_{s1} - and β -casein at a total protein concentration of 1.20 g/dl. Experimental conditions: pH 6.6, barbiturate buffer of 0.1 ionic strength and 2°C.

a. Field strength 3.05 V/s; picture taken after 4800 s;

b. Field strength 1.00 V/s; picture taken after 14400 s.

First, according to LONGSWORTH (1942).

$$\rho = \frac{\sum_i O_i - O_\delta}{\sum_i O_i - O_\epsilon} \quad (2.2)$$

where $\sum O_i$ is the total diagram area and O_δ and O_ϵ that of the δ - and ϵ -boundaries. The average value of ρ found in this way from the patterns in Figure 2.1 was 0.84.

Secondly, we gradually suppressed the δ - and ϵ -boundaries by diluting the protein solution with respect to the electrophoresis buffer (WIEDEMANN, 1947). Extrapolation of the decreasing δ -areas in Figures 2.2a, 2.3a and 2.3b to zero area then also yields $\rho = 0.84$ which is demonstrated in Figure 2.4.

Sedimentation patterns of a 1:1 mixture of α_{s1} - and β -casein under the same experimental conditions as those used with electrophoresis are presented in Figure 2.5. Rapid re-equilibration is suggested by the fact that between the peaks the schlieren pattern does not come back to the base line (GILBERT and JENKINS, 1959).

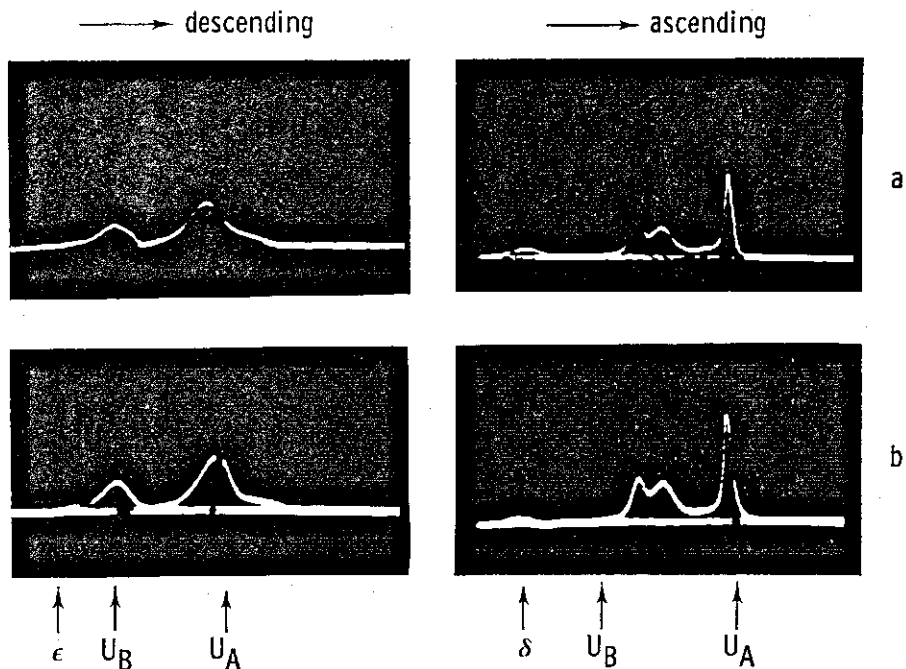


FIG. 2.3 Free electrophoresis of a 1:1 mixture of α_{s1} - and β -casein at a total protein concentration of 1.20 g/dl. Experimental conditions: pH 6.6, barbiturate buffer of 0.1 ionic strength (electrophoresis buffer) and 2°C. Pictures taken after 4800 s. Ratio ionic strength of electrophoresis to dialysis buffer: a. 1.10; b. 1.15.

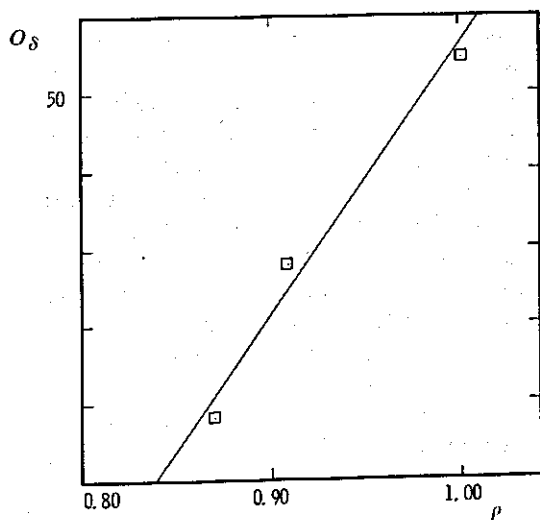


FIG. 2.4 Relationship between dilution factor (ρ) and area of the δ -boundary (arbitrary units). Meded. Landbouwhogeschool Wageningen 74-2 (1974)

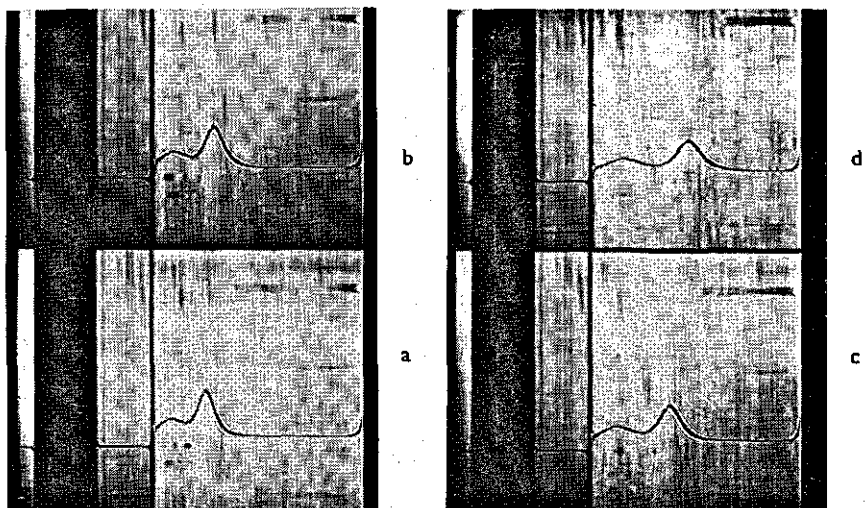


FIG. 2.5 Sedimentation patterns of a 1:1 mixture of α_{s1} - and β -casein at a total protein concentration of 1.20 g/dl. Experimental conditions: barbiturate buffer pH 6.6 and 0.1 ionic strength, 3°C; 50,000 rpm. Pictures taken after: a. 107 min; b. 122 min; c. 152 min; d. 183 min.

The sedimentation coefficient $s_{20,w}$ of the leading peak was found to be 4.5 S, whereas that of the trailing boundary is 1.5 S.

2.4. DISCUSSION

The non-enantiographic patterns presented in Figures 2.1–2.3 and the mobilities and percentages recorded in Table 2.1 afford good evidence, that α_{s1} - and β -casein interact to form complexes of intermediate mobility. The overlap of the patterns at different field strengths (cf. Figure 2.2) is consistent with the idea of rapid re-equilibration during electrophoretic transport (NICHOL et al., 1964; GILBERT and JENKINS, 1959). It is worthy of note, that already KREJCI et al. (1941 and 1942) suspected that the anomalous electrophoretic behaviour of total casein is due to the interaction of its components.

It is instructive to analyse the velocities and areas of the various peaks by the moving boundary theory developed by LONGSWORTH for electrophoresis (1959) and applied by others to similar situations in sedimentation and gel filtration (SCHACHMAN, 1959; NICHOL and WINZOR, 1964).

In the notation introduced by LONGSWORTH (1959) the α_{s1} -casein concentration C_A^c (w/v) under the leading ascending peak is given by

$$C_A^c = \bar{C}_A \frac{\bar{U}_A^b - \bar{U}_B^b}{\bar{U}_A^c - \bar{U}_B^b} \quad (2.3)$$

In this equation \bar{C}_A^b represents the constituent concentration of α_{s1} -casein in the b -solution, defined as

$$\bar{C}_A^b = \sum_i C_{A_i}^b + \sum_j \sum_k \frac{jM_A}{jM_A + kM_B} C_{A_j B_k}^b, \quad (2.4)$$

where M_A and M_B are the molecular weights of α_{s1} - and β -casein, which have been established as 23,000 (SCHMIDT, 1970) and 24,000 (NOELKEN and REIBSTEIN, 1968) respectively. Further, U_A^c is the velocity of pure α_{s1} -casein in the c -solution and \bar{U}_A^b is the constituent velocity of that component in the b -solution and defined as

$$\bar{U}_A^b = \left\{ \sum_i C_{A_i}^b U_{A_i}^b + \sum_j \sum_k \frac{kM_A}{jM_A + kM_B} C_{A_j B_k}^b U_{A_j B_k}^b \right\} / \bar{C}_A^b \quad (2.5)$$

a corresponding definition holds for the constituent velocity \bar{U}_B^b , and it can be shown (LONGSWORTH, 1959) that

$$\bar{U}_B^b = V^{bc} \quad (2.6)$$

where V^{bc} is the volume swept through by the bc -boundary per unit time.

Similarly, for the concentration of pure β -casein under the trailing descending peak we have:

$$C_B^\beta = \bar{C}_B^\alpha \frac{\bar{U}_A^\alpha - \bar{U}_B^\alpha}{\bar{U}_A^\alpha - \bar{U}_B^\beta} \quad (2.7)$$

with

$$\bar{U}_A^\alpha = V^{\alpha\beta} \quad (2.8)$$

The velocities occurring in Equations 2.3 and 2.7 are approximated as follows: \bar{U}_A^b is calculated from the maximum gradient velocity of the leading descending peak by:

$$\bar{U}_A^b = \bar{U}_A^\alpha / \rho^*;$$

\bar{U}_B^b is averaged over the maximum gradient velocities of the ascending bimodal peak and \bar{U}_B^α is found from:

$$\bar{U}_B^\alpha = \bar{U}_B^b \rho^*.$$

The pure component velocities U_A^c and U_B^p are the average values from Table 2.1.

We are now able to compare the experimental areas of the leading ascending

* It can readily be calculated that changes in the constituent mobilities due to shifts of the association equilibria in the δ -boundary are negligible.

TABLE 2.2. Comparing observed and computed pure component peak areas in the electrophoresis of interacting α_{s1} - and β -casein.

mixing ratio α_{s1}/β	velocities (10^{-5} cm/s)						% leading ascending		% trailing descending	
	\bar{U}_A^a	\bar{U}_B^b	b_B	\bar{U}_B^a	U_A^c	U_B^b				
	obs.	calc.		obs.	calc.		obs.	calc.	obs.	calc.
50/50	18.5	22.1	14.4	12.1	24.8	7.5	32	37	28	29
70/30	20.3	24.3	16.1	13.4	25.9	8.9	53	58	14	18

and trailing descending peaks with the computed C_A^c and C_B^b from Equations 2.3 and 2.7. The results are given in Table 2.2, from which it is seen that the calculated areas compare fairly well with the observed ones. It should also be noticed from this table that the leading ascending peaks cover as much as 70% of the *A*-component, whereas on the descending side the trailing peaks contain about 50% of the *B*-component. It is evident from Equations 2.3 and 2.7 that these abnormally high percentages are due to a relatively high constituent velocity \bar{U}_A which in turn suggests that complexes of a high stoichiometric ratio *A/B* dominate among the complexes (cf. Equation 2.5). The presence of higher complexes was already indicated by preliminary GILBERT-type computations in an earlier attempt to reproduce the bimodal reaction boundary (PAYENS, 1968).

CHUN (1965) has analysed the ultracentrifugal pattern of mixture of α_{s1} - and β -casein, assuming the formation of a 1:1 complex of depolymerized α_{s1} - and β -casein with the aid of the theory developed by GILBERT (1959). Several objections can be made to his treatment however. First, the sedimentation method is much less sensitive in discriminating interaction than free electrophoresis, since only a descending boundary is available. More serious, however, is the fact that under the experimental conditions α_{s1} -casein is highly polymerized (SCHMIDT, 1970) and consequently the interaction between the α_{s1} -casein polymers and the β -casein monomer should also be considered.

The sedimentation pattern presented in Figure 2.5 is also indicative of the presence of higher complexes. The slower sedimentation coefficient (1.5 S) corresponds to the monomer of β -casein and the monomer of α_{s1} -casein which have comparable sedimentation coefficients (SCHMIDT et al., 1967). From these values it is readily calculated that the 1:1 complex of monomers, if it were spherical could have a sedimentation coefficient of 2.4 S at the atmost. This is far below the experimental value of 4.5 S found for the rapid peak in Figure 2.5. It should further be realized that in re-equilibrating systems the sedimentation of this faster peak is always slower than that of the complex itself (GILBERT and JENKINS, 1959), which indicates that the complexes present must consist of at least four subunits.

We are now able to roughly qualify the association equilibria which occur under the experimental conditions of electrophoresis.

As is shown by PAYENS and VAN MARKWIJK (1963) β -casein, on account of

the low temperature, will be completely depolymerized. On the other hand, it can be obtained from SCHMIDT's work (1970) that α_{s1} -casein, under the experimental conditions will be polymerized consecutively at least up to the hexamer. Among the complexes formed between α_{s1} - and β -casein those of stoichiometry A_jB ($j > 1$) will predominate.

This conclusion was confirmed by computer simulation of the bc - and $\alpha\beta$ -reaction boundaries. A preliminary account of the simulation method was given earlier (NIJHUIS and PAYENS, 1972) and a more detailed account is presented in the subsequent chapters.

The parameters introduced in the computations were obtained as follows:

1. the polymerization constants and electrophoretic mobilities of α_{s1} -casein were taken from SCHMIDT's (1970) and this work; notably SCHMIDT (1970) observed that α_{s1} -monomers and -polymers have equal mobilities;
2. the A_jB -complex mobilities were calculated by linear interpolation between the pure component mobilities; it is a fortunate coincidence that the computations are rather insensitive to the actual values accepted for the complex mobilities;
3. the equilibrium constants for the complex formation were defined as

$$K_j = C_{A_jB}/C_{A_j}C_B$$

and, since the caseins interact through hydrophobic bonding (SCHMIDT, 1970; PAYENS and VAN MARKWIJK, 1963; VON HIPPEL and WAUGH, 1955), initial K_j -values are chosen so as to compare with the polymerization constants given by SCHMIDT (1970) for pure α_{s1} -casein polymerization.

In accordance with the previous experience of PAYENS (1968), the computations demonstrate clearly that bimodality of the bc -boundary could be produced only if complexes A_jB with $j > 1$ were taken into account. Moreover, it was observed that the agreement between the experimental and computed mobilities and percentages improved if more weight was given to the higher A_jB -complexes. This led us to introduce six parameters for the interactions between all kinds of α_{s1} -polymers and the β -monomer. It is realized that the introduction of so many parameters in the computations certainly will not provide a unique solution. The point of interest is, however, that only the consideration of these multiple equilibria yield the observed bimodal bc -boundaries and mobilities and percentages in agreement with the large constituent velocity \bar{U}_A arrived at before. Some typical simulation results are collected in Table 2.3 and in Figures 2.6 and 2.7.

It is seen that the computed mobilities and percentages compare satisfactorily with the experimental values. We do not consider further refinements of these calculations warrantable for the following reasons.

Firstly, as may be noted from a comparison of Figure 2.6 with Figure 2.7, variations in the interaction parameters do not significantly influence the results of the computations once the existence of the higher complexes has been accepted. Of course this implies that such computations will never yield unique values for the equilibrium constants.

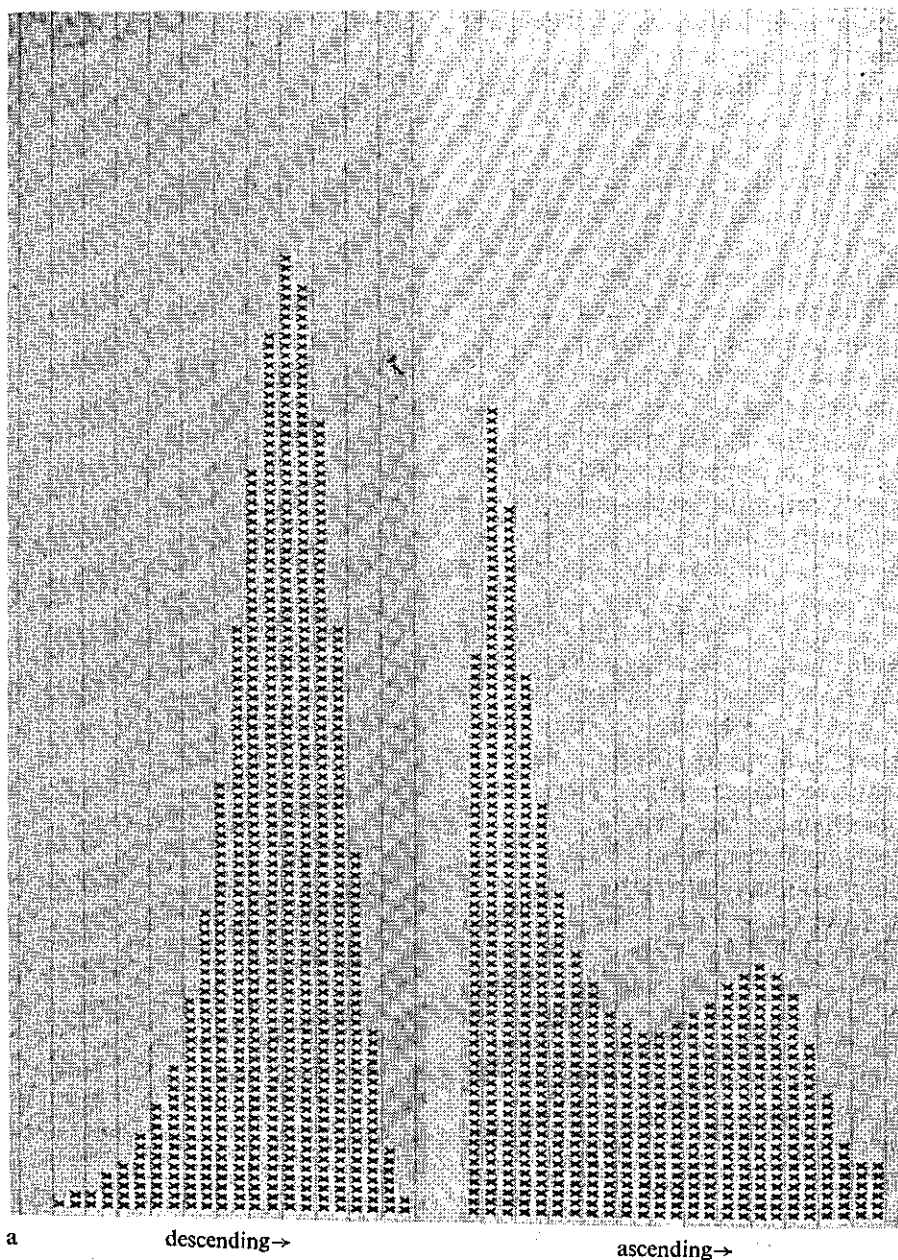
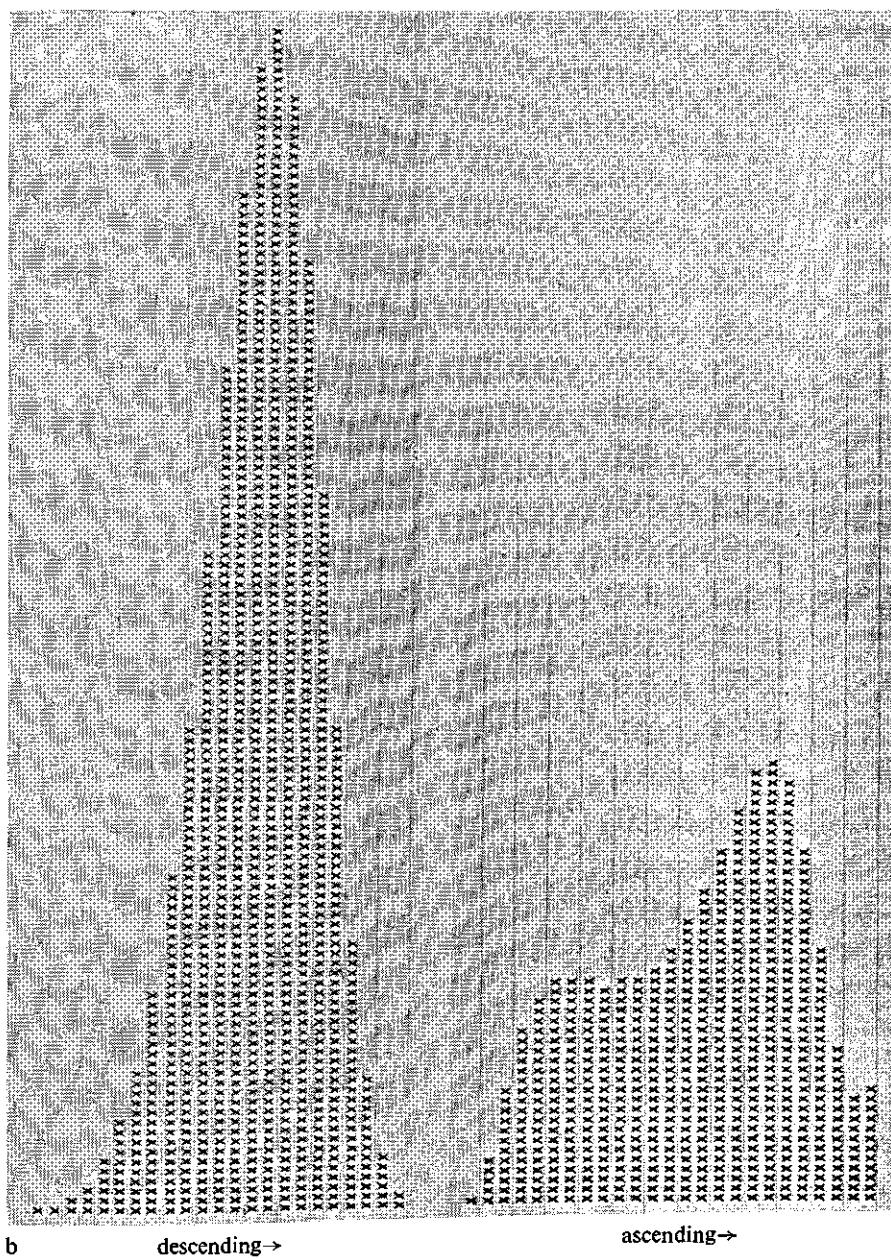


FIG. 2.6 Simulated bc - and $\alpha\beta$ -reaction boundaries for complex forming α_1 - and β -casein during electrophoresis.

Parameters: $K_1 = 10$, $K_2 = 15$, $K_3 = 50$, $K_4 = 100$, $K_5 = 150$, $K_6 = 100$ (g/dl).

Average diffusion coefficients varying from $1-5 \cdot 10^{-7}$ (cm^2/s) (see chapter 3 and 4).

Mixing ratio: a. $\alpha_1/\beta = 50/50$; b. $\alpha_1/\beta = 70/30$.



b

descending →

ascending →

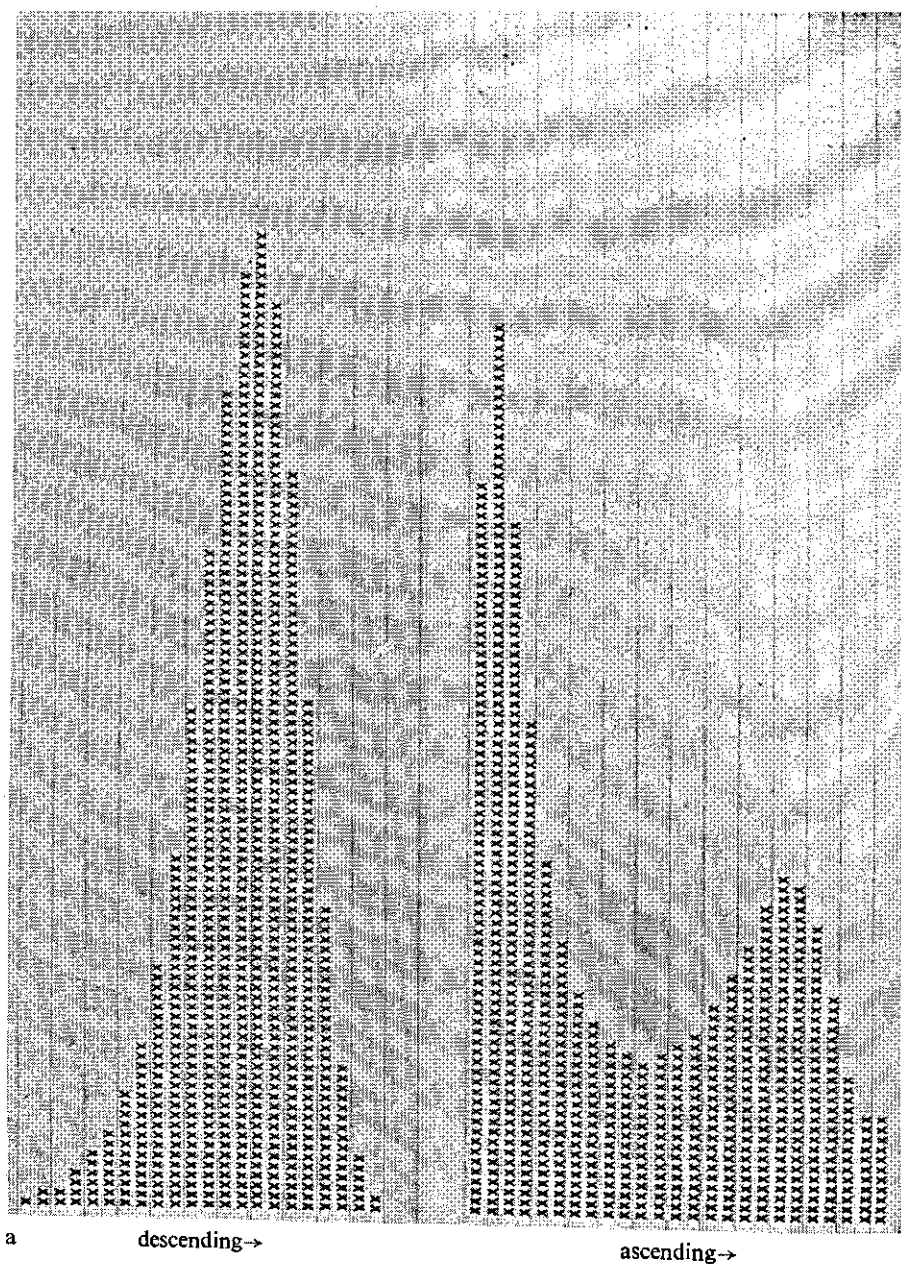


FIG. 2.7 Simulated bc - and $\alpha\beta$ -reaction boundaries for complex forming α_{s1} - and β -casein during electrophoresis.

Parameters: $K_1 = 10$, $K_2 = 25$, $K_3 = 100$, $K_4 = 200$, $K_5 = 300$, $K_6 = 200$ (g/dl).

Average diffusion coefficients varying from $1-5 \cdot 10^{-7}$ (cm^2/s) (see chapter 3 and 4).

Mixing ratio: a. $\alpha_{s1}/\beta = 50/50$; b. $\alpha_{s1}/\beta = 70/30$.

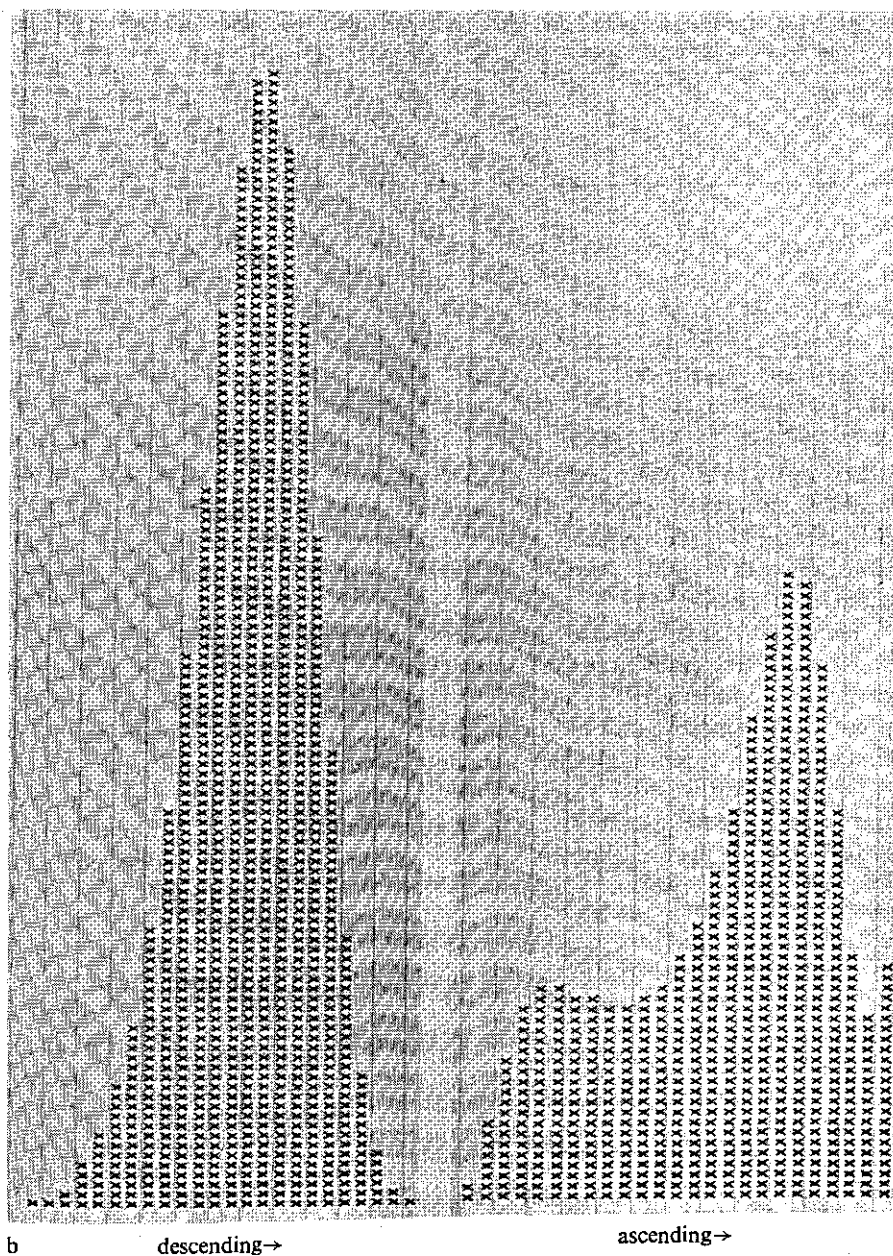


TABLE 2.3. Comparing simulated and experimental reaction boundaries for complex forming α_{s1} - and β -casein during electrophoresis.

mixing ratio α_{s1}/β		ascending			descending	
		velocities (10^{-5} cm/s)		relative area	velocities (10^{-5} cm/s)	relative area
50/50	Fig. 2.5	10.8	20.0	63.6	17.7	64.2
	Fig. 2.6	10.8	21.2	64.2	17.6	64.8
	Exptl. ¹	12.7	16.9	68	18.5	72
	Fig. 2.5	13.8	20.9	51.9	18.1	86.2
70/30	Fig. 2.6	13.1	21.7	54.6	18.0	78.4
	Exptl. ¹	13.9	18.9	47	20.2	86

¹Average values from Table 2.1.

Secondly, as a consequence of the KOHLRAUSCH-SVENSSON effect the faster peaks are always enlarged at the cost of the slower ones (LONGSWORTH, 1959; SVENSSON, 1946). This effect has not been accounted for in the present calculations, since its magnitude is difficult to evaluate in systems containing more than three ionic species.

Thirdly, on close inspection the electrophoretic patterns of Figures 2.1 to 2.3 show a non-zero gradient in the *b*-phase, and sometimes a minor shoulder ahead of the $\alpha\beta$ -boundaries. It is suspected that these abnormalities are due to the presence of minor quantities of complexes which have a mobility approaching that of pure α_{s1} -casein, and which were not accounted in the present calculations.

In conclusion we state that the interaction between α_{s1} - and β -casein gives rise to an intricate assembly of complexes in which α_{s1} -casein dominates. This is in line with the well-known tendency of these proteins to form colloidal micelles in milk (WAUGH, 1971).

III COMPUTER SIMULATION OF ELECTROPHORETIC EXPERIMENTS

3.1. INTRODUCTION

Transport techniques such as electrophoresis, ultracentrifugation and gel filtration can be used to advantage in studying biopolymer interactions (GILBERT and JENKINS, 1959; CANN and GOAD, 1970; NICHOL et al., 1964; ACKERS, 1970; ZIMMERMAN and ACKERS, 1971; ZIMMERMAN et al., 1971; HENN and ACKERS, 1969; THOMPSON and ACKERS, 1965; NICHOL and WINZOR, 1964; WINZOR and SCHERAGA, 1963). Several methods have been proposed to solve the conservation-of-mass equation for a system of interacting biopolymers in transport experiments. GILBERT (1959) and GILBERT and JENKINS (1959) have presented analytical expressions for the concentration and the concentration gradient in polymerizing and complex forming systems neglecting the effect of diffusion on the spreading of a boundary. The usefulness of this approach resides in the fact that in prolonged experiments the contribution of diffusion often can be neglected when compared to the spreading caused by the differential migration of the different polymer species. It is realized, however, that in experiments of finite duration and/or with the occurrence of small peaks or shoulders, it may be important to assess the blurring effect of the diffusion on the shape of a boundary. This has led a number of authors to solve the complete conservation-of-mass equation by numerical or simulation methods (CANN and GOAD, 1970; COX, 1965A, 1965B, 1967, 1969, 1971A, 1971B; BETHUNE, 1970).

COX for instance (1969, 1971A, 1971B) simulated the sedimentation pattern of polymerizing proteins by taking into account the non-uniform ultracentrifugal field and radial dilution of the protein. Essentially, in this method the ultracentrifuge cell is divided into a large number of small segments the leading edges of which are displaced with the weight-average sedimentation coefficient of the protein present in the segment on the upstream side of that edge. This transport cycle is followed by a diffusion step during an equal interval of time. Successive alternate rounds of sedimentation and diffusion permit the simulation of concentration-dependent ultracentrifugation, be it as a consequence of polymerization or hydrodynamic interaction.

CANN and GOAD (1970) solved the complete conservation-of-mass equation by considering the contributions of the individual species to the fluxes due to velocity and diffusional transport. Also in this approach the boundary is divided into a large number of segments and the flux at a particular segment edge is calculated from the average concentrations in a number of neighbouring boxes. Equilibrium between the individual species is re-established after each transport cycle. Actually the flux at a particular edge is related to the average concentration in all boxes. GOAD showed that if the velocity flux is

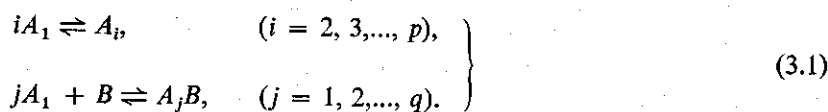
restricted to the transfer of material from one box to the next a diffusion-like error is introduced. This author therefore preferred to suppress this error by taking into account the contribution of the average concentrations of several boxes to the flux and to introduce the diffusional flux separately. This is certainly a most accurate procedure, but it will be demonstrated below that for practical purposes the diffusion-like error can be used to simulate the diffusional flux, which leads to a drastic reduction of the computations.

Still another approach to simulate boundaries in transport experiments was introduced by BETHUNE and KEGELES (1961A, 1961B, 1961C), who stressed the analogy of the equations governing the countercurrent distribution process with those describing the problem at hand. BETHUNE (1970) has simulated the boundary spreading of self-associating and complex forming polymers during electrophoresis and sedimentation and compared his results with the asymptotic solutions given by GILBERT (1959). BETHUNE (1970) also has discussed the proper choice of the countercurrent distribution coefficient in order to account quantitatively for the diffusional effect in polymerizing systems.

The method of simulation presented in this chapter is – as stated above – a simplification of the procedure outlined by CANN and GOAD (1970). It will be shown that the method also carries a close relationship to the countercurrent simulation approach of BETHUNE and KEGELES (1961A, 1961B, 1961C). Application of the method to the simulation of the anomalies observed during the electrophoresis of complex forming α_{s1} - and β -casein has already been presented in Chapter 2.

3.2. THEORY OF THE SIMULATION METHOD AND DISCUSSION OF THE RESULTS

Let us consider the following system of interacting biopolymers A and B :



The complex formation between α_{s1} - and β -casein at the temperature of free electrophoresis and the interaction between RNA and virus coat protein (DURHAM et al., 1971) offer among others (NICHOL et al., 1964) excellent examples of such a system.

The computation of the equilibrium concentrations of the various species requires the solution of the following set of equations

$$K_i = A_i/A_1^i, \quad (i = 2, 3, \dots, p) \quad (3.2)$$

$$L_j = A_jB/(A_1^jB), \quad (j = 1, 2, \dots, q) \quad (3.3)$$

$$\bar{A} = \sum_{i=1}^p A_i + \sum_{j=1}^q (1-\lambda_j)A_jB \quad (3.4)$$

$$\bar{B} = B + \sum_{j=1}^q \lambda_j A_j B \quad (3.5)$$

In these equations K_i and L_j represent the equilibrium constants for the self-association of A and for the complex formation between A and B respectively, \bar{A} and \bar{B} stand for the constituent concentration (w/v) of A and B and λ_j is defined as

$$\lambda_j = M_B / (jM_A + M_B)$$

with M_A and M_B the monomer molecular weights of A and B . Equations 3.2 – 3.5 lead to the following expression for the monomer concentration of component A :

$$\left(\sum_{i=1}^p K_i A_1^i \right) \left(\sum_{j=0}^q \lambda_j L_j A_1^j \right) + \sum_{j=0}^q \left[\{ \bar{B} - (\bar{A} + \bar{B}) \lambda_j \} L_j A_1^j \right] = 0 \quad (3.6)$$

with $K_1 = L_0 = 1$.

Equation 3.6 is a polynomial in the monomer concentration A_1 , the graphical appearance of which is shown in Figure 3.1. In the computation of the equilibrium concentration, A_1 is found by NEWTON-RAPHSON iteration (MARGENAU

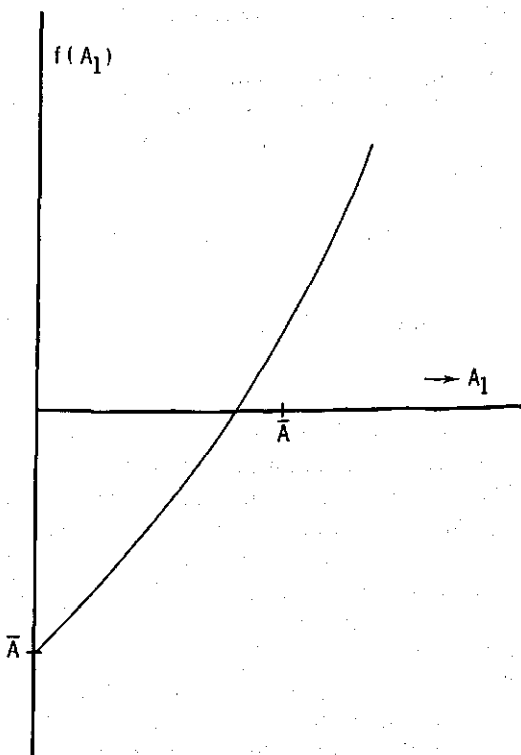


FIG. 3.1 Schematic plot of the polynomial (Equation 3.6) used for the computation of the monomer concentration (A_1) of component A .

and MURPHY, 1955). The constituent concentration \bar{A} , being the highest possible value of A_1 , appears to be a natural starting value for the iteration. Actually, however, the number of iteration steps can be reduced considerably by estimating the starting value of A_1 in a particular box from its concentration in the preceding one (see Chapter 4.).

The simulation of the free electrophoresis of a system of interacting biopolymers is achieved by subdividing the electrophoretic channel into a large number of small boxes of equal length Δx . The development of the reaction boundaries is brought about by alternate rounds of velocity transport of the individual species from one box to the next during an interval of time Δt , followed by re-equilibration according to Equation 3.2 – 3.5.

On the ascending side velocities are taken relative to the slowest species (i.e. component B) and the ratio $\Delta x/\Delta t$ is chosen such that the fastest component just reaches the end of a box, therefore

$$V_A - V_B = \Delta x/\Delta t. \quad (3.7)$$

The complexes, having intermediate mobilities, penetrate the boxes only partially. Similarly on the descending side the velocities are changed of sign and taken relative to the component with the highest absolute value of the electrophoretic mobility (i.e. component A).

The source program for the simulation, a flow scheme of which is presented in Figure 3.2, was written in ALGOL-60. All computations have been carried out on the CDC-3200 digital computer complex of the Agricultural University.

It is worth while to analyse the above simulation procedure somewhat further.

With the $(n+1)^{\text{th}}$ transfer, the change of mass in box r due to component i is given by

$$\Delta m_{r,n+1}^i = m_{r,n+1}^i - m_{r,n}^i = f_i (m_{r-1,n}^i - m_{r,n}^i), \quad (3.8)$$

$$\text{where } f_i = v_i \Delta t/\Delta x$$

and v_i is the relative velocity of species i , $v_i - v_B$. Obviously, from our choice of reference of the relative velocities and of $\Delta t/\Delta x$ (Equation 3.7), we have $0 < f_i < 1$.

The mass transfer of each species from one box to the next is thus seen to be determined by a constant fraction f_i of the mass difference between adjacent boxes. This transfer is therefore found to be identical with the mass transfer taking place in the countercurrent distributional process. In the latter case we have $f_i = P_i/(P_i + 1)$, where P_i is the partition coefficient of the species i (CRAIG and CRAIG, 1950). As mentioned in the introduction, BETHUNE and KEGELES (1961A, 1961B, 1961C) and BETHUNE (1970) have used the mass distribution achieved in a continuous countercurrent process to account for the effect of the diffusional spreading on the transport pattern of interacting proteins. It is worth noting, however, that the countercurrent analog involves more computations than the present method of simulation, since it requires not only

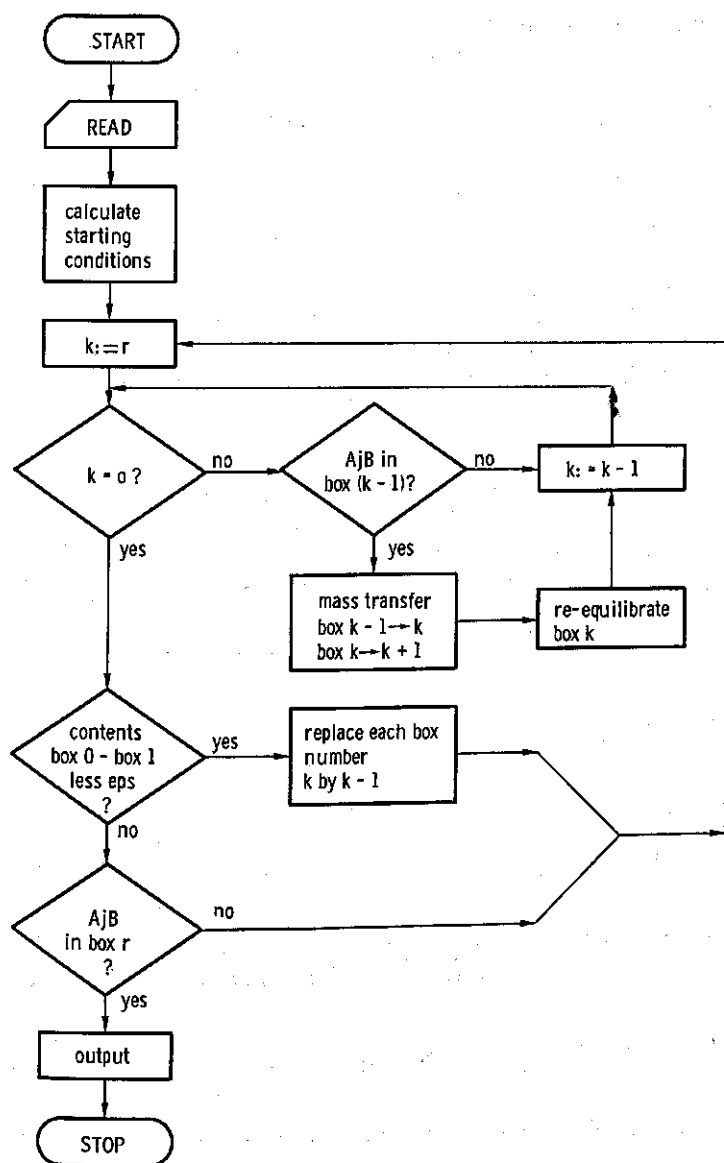


FIG. 3.2 Flow diagram for the simulation of reaction boundaries of complex forming proteins in transport experiments.

the computation of the partition equilibrium but also those of the chemical equilibria in both the upper and lower layer of each countercurrent tube.

Following BETHUNE (1970) we thus find for the mass distribution of species i after a sufficiently large number of transfer cycles n :

$$\partial C_{ii} / \partial n = \frac{1}{2} f_i (1 - f_i) \partial^2 C_{ii} / \partial r^2 - f_i \partial C_{ii} / \partial r, \quad (3.10)$$

where r is box number and C_i is the concentration of species i in g/dl. Similarly, for the mixture of interacting biopolymers we have

$$\partial \sum_i C_i / \partial n = \partial^2 \left\{ \sum_i \frac{1}{2} f_i (1-f_i) C_i \right\} / \partial r^2 - \partial \sum_i f_i C_i / \partial r \quad (3.11)$$

If now – following again BETHUNE and KEGELES – we draw the following analogies:

$n \leftrightarrow t$ and $r \leftrightarrow x$,

then Equations 3.10 and 3.11 show the formal analogy with the complete conservation-of-mass equation in transport experiments in which the distance is expressed in units of length Δx and time in units Δt . As a consequence the simulated diffusion coefficients of component i , expressed in cm^2/s , becomes

$$D_i^* = \frac{1}{2} f_i (1-f_i) (\Delta x)^2 / \Delta t. \quad (3.12)$$

In systems containing three migrating components atmost the D_i^* values can generally adepted individually by a proper choice of Δx , Δt and f_i , as will be demonstrated in the next section. However, in the present case, dealing with more components only the simulated average diffusion coefficient can approximately brought into agreement with the actual value.

In the mixture of biopolymers the actual diffusion flux is defined by (Cox, 1969):

$$J_D = \bar{D} \sum_i (\partial C_i / \partial x), \quad (3.13)$$

where \bar{D} is the gradient averaged diffusion coefficient

$$\bar{D} = \sum_i [D_i \partial C_i / \partial x] / \sum_i [\partial C_i / \partial x] \quad (3.14)$$

and D_i is the true diffusion coefficient of component i . In accordance with Equation 3.12 the simulated gradient averaged diffusion coefficient, expressed in cm^2/s , becomes

$$\bar{D}^* = \left[\sum_i \left\{ \frac{1}{2} f_i (1-f_i) \partial C_i / \partial r \right\} / \sum_i \{ \partial C_i / \partial r \} \right] (\Delta x)^2 / \Delta t \quad (3.15)$$

The adjustment of the simulated to the actual diffusion coefficient now demands that we put

$$\bar{D}^* = \bar{D}. \quad (3.16)$$

Equations 3.14–3.16 and 3.7 show that Δx and Δt are fixed by the values of the relative velocities, the diffusion coefficients D_i and the concentration gradients $\partial C_i / \partial x$. The latter will be discussed below. The number of transfer cycles, n , which is necessary for the simulation of a particular reaction boundary, finally follows as the ratio of the time of the experiment and Δt . Conversely in the simulation of a given experiment an arbitrary choice of n determines

together with the duration of the experiment an arbitrary Δt . The corresponding Δx then follows from Equation 3.7 and the diffusional spreading operative in this simulation from Equation 3.15. It is obvious that in general then \bar{D}^* will not equal \bar{D} .

We are now able to elaborate upon the simulation of complex forming α_{s1} - and β -casein dealt with in the previous chapter.

Since we have no a priori knowledge of the concentration gradients $\partial c_i / \partial x$ existing in the reaction boundaries, we must start with a comparison of the simulated patterns computed for arbitrary numbers of transfer. Typical results of the simulation of the ascending electrophoretic pattern of a 1:1 mixture of α_{s1} - and β -casein for $n = 27, 46, 73$ and a duration of the experiment of 4800 s are presented in figures 3.3a–3.3c, from which it is seen, that the general appearance of the pattern is not affected substantially by the number of transfers. More importantly, as is seen from Table 3.1, also the maximum and minimum gradient mobilities and the concentration changes over the reaction boundary do not change appreciably with n . This result, of course, is in agreement with GILBERT and JENKINS' conclusion (1959) that in prolonged experiments the effect of diffusional spreading on a boundary is negligible. In other words: the proper choice of the number of transfers is of minor importance for a correct simulation of the percentages and mobilities found from experimental electrophoretic patterns.

The calculations underlying Table 3.1 and Figure 3.3 also yield the concentration gradients necessary for a comparison of the averaged true and simulated diffusion coefficients defined by Equations 3.14 and 3.15. To this end we have approximated the various $\partial C_i / \partial x$ by the total concentration change of the species i over the boundary. The actual value of \bar{D} is then estimated as follows. From existing data (SCHMIDT, 1970; NOELKEN and REIBSTEIN, 1968) we find the diffusion coefficient, D_1 , of monomeric α_{s1} - and β -casein, corrected for the temperature of free electrophoresis, to be $3.2 \cdot 10^{-7} \text{ cm}^2/\text{s}^*$. The diffusion coefficients of the polymers or complexes containing i subunits are then calcu-

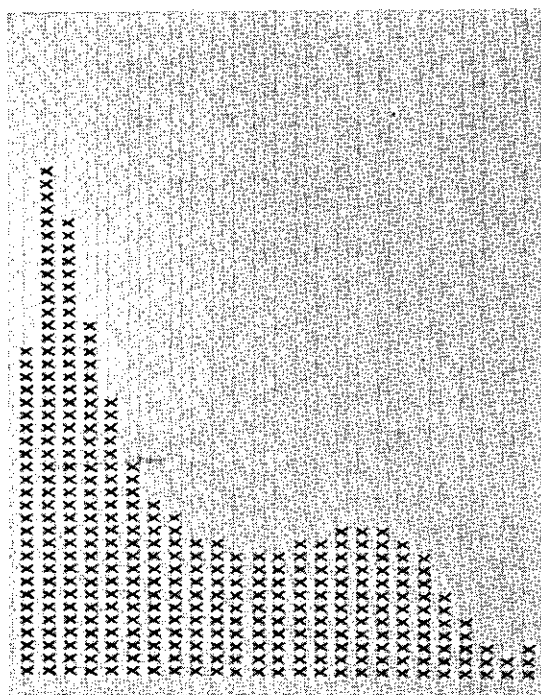
TABLE 3.1. Comparing velocities and percentages of the ascending electrophoretic boundaries of complex forming α_{s1} - and β -casein simulated for different numbers of transfer.

Number of transfers	number of boxes	velocities ¹ (10^{-5} cm/s)			percentages ²		
					A ₁	A ₂	A ₃
27	25	1.96	1.64	1.09	0.30	0.24	0.47
46	40	1.94	1.60	1.08	0.31	0.22	0.47
73	60	1.94	1.58	1.07	0.31	0.22	0.46

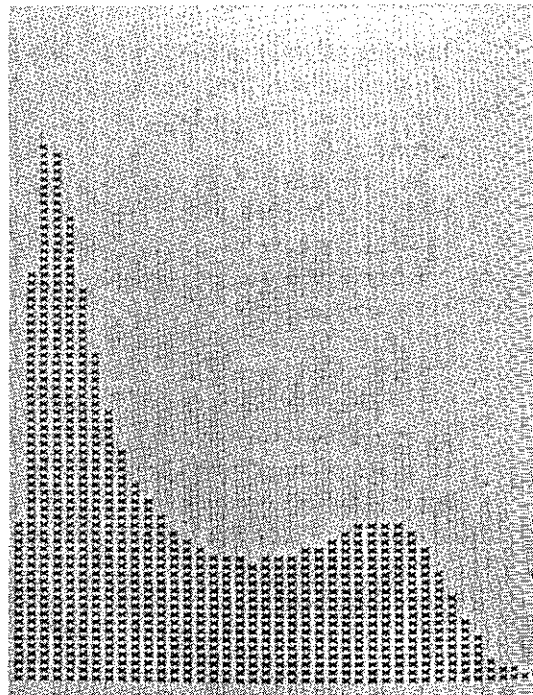
¹ Velocities corresponding to the maximum and minimum gradients of the reaction boundaries.

² A₁ relative area of pure α_{s1} -casein; A₂, A₃, relative areas under bimodal peak.

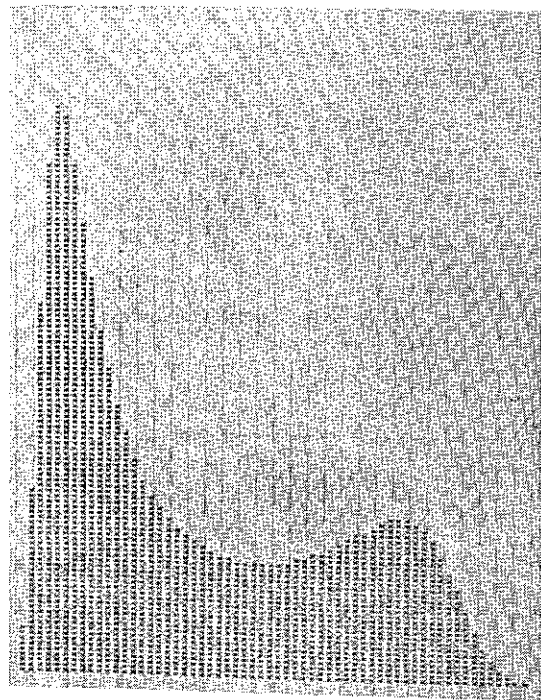
* The molecular parameters of monomeric α_{s1} - and β -casein are almost the same (SCHMIDT, 1970; NOELKEN and REIBSTEIN, 1968).



a



b



c



FIG. 3.3 Simulation of the ascending electrophoretic reaction boundaries for a 1:1 mixture of α_{s1} - and β -casein;
a: number of transfers 27,
b. number of transfers 46,
c. number of transfers 73.

TABLE 3.2. Comparing simulated and true gradient averaged diffusion coefficients pertaining to the computations presented in Table 3.1.

Number of transfers	Δt (s)	Δx (nm)	$\bar{D}^* (\Delta x)^2 / \Delta t$ ($10^{-7} \text{cm}^2/\text{s}$)	$\bar{D} \cdot 10^7$ (cm^2/s)
27	177.8	277.3	3.286	2.527
46	104.3	162.8	1.958	2.534
73	65.8	102.6	1.241	2.536

lated from that of the monomers by the STOKES-EINSTEIN relation:

$$D_i = D_1 i^{-1/3} \quad (3.17)$$

A similar calculation is performed for the estimation of the simulated diffusion coefficient, \bar{D}^* , according to Equation 3.15.

The comparison of the \bar{D} and \bar{D}^* estimated in this way for $n = 27, 46$ and 73 is given in Table 3.2, from which it may be noted that the value of the diffusion coefficient, \bar{D} , is hardly affected by this change of n . The simulated diffusion coefficients \bar{D}^* , however, are found to be inversely proportional to n as expected from the theory presented above. Actually Table 3.2 indicates that the most accurate number of transfers should be about 35, corresponding to an averaged simulated diffusion coefficient of $\bar{D}^* = 2.55 \cdot 10^{-7} \text{ cm}^2/\text{s}$. Similar considerations hold for the simulation of descending electrophoretic or ultracentrifugal patterns.

The above analysis shows the usefulness of the simplified procedure for the simulation of the reaction boundaries observed in the electrophoresis (or ultracentrifugation) of interacting proteins. In agreement with the conclusions arrived at by GILBERT and JENKINS (1959) the value of the average simulated diffusion coefficient, \bar{D}^* , thereby appears to be of minor importance for the reproduction of the experimental peak areas and mobilities. The adjustment of the simulated to the true diffusion coefficient can easily be achieved, however, by carrying out a preliminary computation with an arbitrary number of transfers. From this the true average diffusion coefficient, \bar{D} , is estimated as exposed above. The most realistic number of transfers then follows from the equalization from the true and simulated average diffusion coefficients (Equation 3.16).

3.3. ALTERNATIVE METHODS FOR THE SIMULATION OF DIFFUSIONAL FLUXES

BETHUNE (1970) has presented an alternative procedure for the adjustment of simulated and actual diffusion coefficients for the case of a discrete self-associating system. His treatment can easily be extended to systems containing three components as for example in complex forming systems of the type $A + B \rightleftharpoons C$.

For the simulation of the diffusion of one component it is to be noticed that there are three undetermined parameters i.e. the depth of the box, Δx , the dura-

tion of a transport cycle, Δt , and the fractional transfer parameter f (Equation 3.9). They are interconnected by two equations, viz.

$$v = f\Delta x/\Delta t, \quad (3.17)$$

$$D = \frac{1}{2}f(1-f)(\Delta x)^2/\Delta t. \quad (3.18)$$

Thus we have one degree of freedom in the choice of Δt , Δx and f .

Also in this case the analytical solution of the complete conservation-of-mass equation is available (CRANK, 1967):

$$\frac{\partial C}{\partial r} = \frac{1}{\sqrt{4\pi Dn}} e^{-\left\{\frac{(r-vn)^2}{4Dn}\right\}} \quad (3.19)$$

We are therefore able to compare the results of the simulation procedure treated above with the analytical expression (Equation 3.19). As is shown in Table 3.3 the results obtained from the analytical expression compare satis-

TABLE 3.3. Comparison of exact and simulated schlieren patterns for one migrating component. Simulation parameters: $n = 30$, $f = \frac{1}{2}$, $\Delta t = \Delta x = 1$, corresponding to $D = 1/8$ and $v = \frac{1}{2}$.

box number	$\partial C/\partial r$ simulated	$\partial C/\partial r$ Eqn. 3.19
1	0.0000	0.0000
2	0.0000	0.0000
3	0.0000	0.0000
4	0.0000	0.0000
5	0.0001	0.0002
6	0.0006	0.0007
7	0.0019	0.0020
8	0.0055	0.0056
9	0.0133	0.0132
10	0.0280	0.0275
11	0.0509	0.0501
12	0.0806	0.0799
13	0.1115	0.1116
14	0.1354	0.1363
15	0.1445	0.1457
16	0.1354	0.1363
17	0.1115	0.1116
18	0.0806	0.0799
19	0.0509	0.0501
20	0.0280	0.0275
21	0.0133	0.0132
22	0.0055	0.0055
23	0.0019	0.0020
24	0.0006	0.0007
25	0.0001	0.0002

factorily with those from the simulation procedure. The discrepancies can be explained on the grounds of the analysis given by CANN and GOAD (1970). These authors showed that the relation of the concentration in a certain box and the concentrations at a particular point can be obtained by TAYLOR expansion. From their expression it is seen that our simulation procedure not only introduces a diffusion-like flux but also fluxes of higher order.

For the case of discrete self-association the proper choice of the simulation parameters is straightforward (BETHUNE, 1970). We now have 4 parameters (Δt , Δx , f_M and f_P) which are completely fixed by the four following Equations:

$$v_M = f_M \Delta x / \Delta t, \quad (3.20)$$

$$v_P = f_P \Delta x / \Delta t, \quad (3.21)$$

$$D_M = \frac{1}{2} f_M (1 - f_M) (\Delta x)^2 / \Delta t, \quad (3.22)$$

$$D_P = \frac{1}{2} f_P (1 - f_P) (\Delta x)^2 / \Delta t, \quad (3.23)$$

where v_M and v_P and D_M and D_P denote the velocities and diffusion coefficients of monomer and polymer respectively. The solution of this set of equations is achieved in two stages.

First, $\Delta x / \Delta t$ and $(\Delta x)^2 / \Delta t$ are eliminated from the Equations 3.20–3.23. In this way the ratio of the diffusion coefficients and the ratio of the velocities are brought into agreement with the simulated ones. Since D_M and D_P are parabolic functions of f_M and f_P , whereas v_M and v_P are linear dependent on f_M and f_P the above procedure is equivalent to finding the proper set of (x, y) -values on the parabola relating the simulated diffusion coefficient and the velocity parameters f_M and f_P (Figure 3.4a).

Next, for one component (e.g. monomer) the simulated diffusion coefficient and the simulated velocity are scaled by calculating the proper Δx and Δt from Equations 3.20 and 3.21 with the value found for f_M . It is easy to show that f_M , f_P , Δx and Δt are given by

$$f_M = \frac{\frac{D_P}{D_M} - \frac{v_P}{v_M}}{\frac{D_P}{D_M} - \left(\frac{v_P}{v_M}\right)^2} \quad (3.24)$$

$$f_P = \frac{\frac{D_M}{D_P} - \frac{v_M}{v_P}}{\frac{D_M}{D_P} - \left(\frac{v_M}{v_P}\right)^2} \quad (3.25)$$

$$\Delta x = 2 \frac{v_M D_P - v_P^2 D_M / v_M}{v_M v_P - v_P^2} \quad (3.26)$$

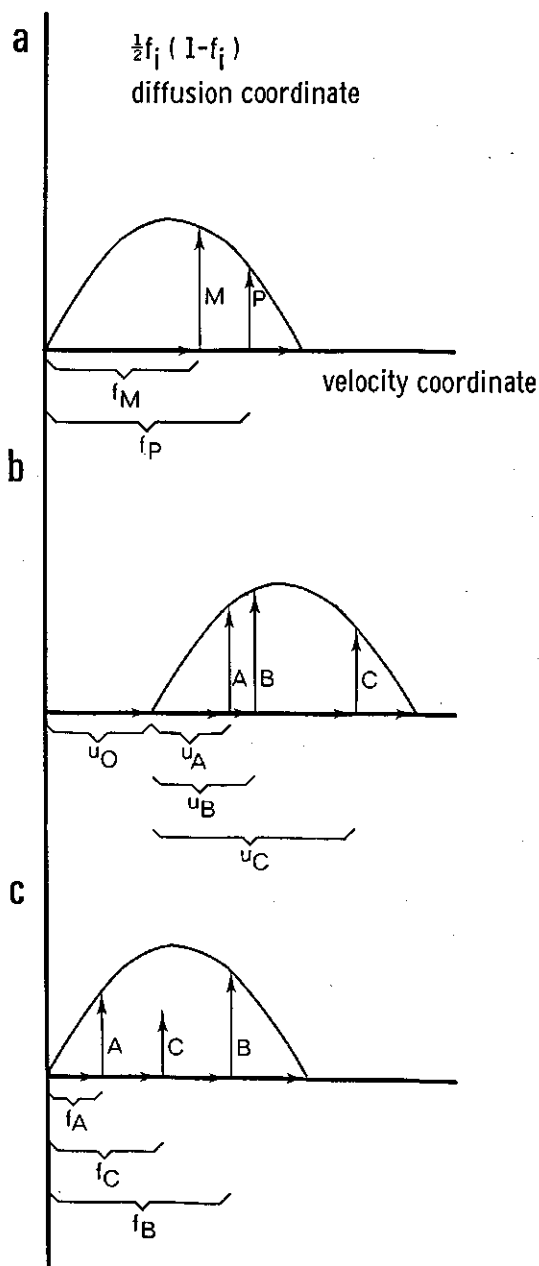


FIG. 3.4 Schematic picture of the adjustment of simulated diffusion coefficients and simulated velocities;

a. discrete polymerization: $M(\text{onmer}) \rightleftharpoons P(\text{olymer})$ in the case of gel filtration or ultracentrifugation,

b. complex formation (three components) $A + B \rightleftharpoons C$ in the case of gel filtration or ultracentrifugation,

c. as with b but in the case of electrophoresis.

$$\Delta t = 2 \frac{D_P - v_P D_M / v_M}{v_M v_P - v_P^2} \quad (3.27)$$

In the case of a complex forming system like $A+B \rightleftharpoons C$, the problem arises that five parameters ($\Delta x, \Delta t, f_A, f_B, f_C$) must conform to six Equations:

$$v_i = f_i (\Delta x) / \Delta t, \quad (i = A, B, C), \quad (3.28)$$

$$D_i = \frac{1}{2} f_i (1 - f_i) (\Delta x)^2 / \Delta t, \quad (i = A, B, C). \quad (3.29)$$

This difficulty, however, can be overcome by introducing a sixth parameter: the velocity of the frame, v_O , related to the simulation parameter, u_O , by $v_O = u_O \Delta x / \Delta t$. This causes a new set of fractional transfer parameters, u_i ($i = A, B, C$), which must be used in the simulation procedure defined as

$$u_i = f_i - u_O, \quad (i = A, B, C). \quad (3.30)$$

Now u_i becomes the fraction of mass moving from one box to the next thus $0 < u_i < 1$ ($i = A, B, C$). As is exposed above u_i will then be determinative of the simulated diffusion, whereas f_i still determines the velocity. In this method the simulated velocity and the simulated diffusion are no longer interdependent. Instead of Equations 3.28 and 3.29 we now have

$$v_i = (u_i + u_O) (\Delta x) / \Delta t, \quad (i = A, B, C), \quad (3.31)$$

$$D_i = \frac{1}{2} u_i (1 - u_i) (\Delta x)^2 / \Delta t, \quad (i = A, B, C). \quad (3.32)$$

Eliminating $\Delta x / \Delta t$ and $(\Delta x)^2 / \Delta t$ and putting $v_A / v_B = A$, $v_A / v_C = B$, $D_B / D_A = C$, and $D_C / D_A = D$ a set of Equations is obtained for u_i ($i = O, A, B, C$):

$$A = \frac{u_A + u_O}{u_B + u_O} \quad (3.33)$$

$$B = \frac{u_A + u_O}{u_C + u_O} \quad (3.34)$$

$$C = \frac{u_B (1 - u_B)}{u_A (1 - u_A)} \quad (3.35)$$

$$D = \frac{u_C (1 - u_C)}{u_A (1 - u_A)} \quad (3.36)$$

From Equations 3.33–3.36 the following expressions can be found for u_O, u_A, u_B and u_C :

$$u_A = \frac{1}{2} \pm \frac{1}{2} \sqrt{\frac{-A_1 \pm \sqrt{A_1^2 - 4A_0A_2}}{2A_0}}$$

$$u_B = \frac{1}{2} \pm \frac{1}{2} \sqrt{4Cu_A^2 - 4Cu_A + 1}$$

$$u_C = \frac{(A-B)u_A + A(B-1)u_B}{B(A-1)}$$

$$u_O = \frac{Au_B - u_A}{1-A}$$

where

$$A_0 = S^2 - QDC$$

$$A_1 = 2ST - Q(C+D-2CD)$$

$$A_2 = T^2 - Q(1-C)(1-D)$$

$$S = C \left\{ \frac{A(1-B)}{A-B} \right\}^2 + D \left\{ \frac{B(1-A)}{A-B} \right\}^2 - 1$$

$$T = (1-C) \left\{ \frac{A(1-B)}{A-B} \right\}^2 + (1-D) \left\{ \frac{B(1-A)}{A-B} \right\}^2$$

$$Q = 4 \left\{ \frac{A(1-B)}{A-B} \right\}^2 \left\{ \frac{B(1-A)}{A-B} \right\}^2$$

After u_A , u_B , u_C and u_O have been solved Δt and Δx are found by the scaling procedure described for the two component system. In principle by equations 3.33-3.36 there are 8 sets of solutions. The values found in this way are restricted by the condition $0 < u_i < 1$ ($i = A, B, C$). It should further be kept in mind that there exist pairs of solutions which are symmetrical about $u = \frac{1}{2}$ and the overall transport of which will be opposite. Obviously such a pair may represent the corresponding ascending and descending limbs in free electrophoresis (or gel filtration). If $f_i > 0$ ($i = A, B, C$) we are dealing with the ascending side, whereas for $f_i < 0$ the descending side is simulated.

In the case of gel filtration the fastest component is the complex which has the smallest partition coefficient and diffusion coefficient. It is clear from Figure 3.4b that for this case a fit on the diffusion parabola can also be realized and proper values for u_i ($i = A, B, C$) can be found. The same holds true for the case of ultracentrifugation, provided the conditions mentioned on page 38 are satisfied.

From the electrophoresis of widely different complex forming systems it is

evident that the electrophoretic mobility of the complexes is always intermediate between those of the pure reactants (GILBERT and JENKINS, 1959; CANN and KLAPPER, 1961; THOMPSON and MACKERNAN, 1961). In this case no solution of Equations 3.33–3.35 is available, as is apparent from Figure 3.4c. By considering the average diffusional flux a satisfactory solution can also be found for this case, as was shown above.

IV A PROGRAM IN ALGOL FOR THE SIMULATION OF ELECTROPHORETIC REACTION BOUNDARIES OF INTERACTING BIOPOLYMERS

4.1. CONSTRUCTION OF PROGRAM

The program used for the simulation of reaction boundaries of interacting biopolymers during electrophoresis was written in ALGOL-60. Input and output procedures were adopted according to the conventions proposed in ALGOL-60, as published by NAUR et al. (1963). The program was adapted to the Control Data 3200 Computer of the Computer Centre of the Agricultural University at Wageningen.

The simulation programs for the ascending and descending electrophoretic patterns were named ASC-PQ and DESC-PQ respectively. The programs are also applicable to the rising and descending boundaries in gel filtration experiments with existing plateau region (WINZOR and SCHERAGA, 1963). The program DESC-PQ can also be applied to sedimentation of interacting macromolecules provided the influences of the non-uniformity of the centrifugal field and radial dilution effects (SCHACHMAN, 1959) may be neglected.

The main differences between these programs ASC-PQ and DESC-PQ were: first, the way in which the starting conditions were calculated; second, the manner in which the output is presented. The flow scheme (Figure 3.2) of both programs, however, is the same. The successful operation of the simulation program demands that special attention should be paid to the following facts.

1. According to the transfer Equation 3.8 new concentrations in a given box after each transfer cycle are governed by the concentrations in that box and the preceding one before transfer. The transfers in a particular round should not influence each other. It is therefore necessary to carry out the successive transfers in upstream direction.
2. After each transfer the new equilibrium concentrations are calculated. This calculation consists of three steps:

First, the coefficients of the polynomial Equation 3.6 are calculated.

Second, the monomer concentration A_1 is found as the real and positive root of Equation 3.6 by NEWTON-RAPHSON iteration (MARGENAU and MURPHY, 1955). Third, the new concentrations of all components are calculated from A_1 with the aid of Equations 3.2 and 3.3 and the accepted values for the various equilibrium constants.

It is advantageous to reduce the number of iteration steps in the computation of A_1 , since this part of the program is repeated mostly. Therefore a starting value for A_1 is chosen close as possible to its final value reached in the iteration. In this respect it should also be borne in mind that the degree of convergence of the NEWTON-RAPHSON iteration diminishes when the degree of the polynomial

increases. As an example in the present case of α_{s1} - and β -casein complex formation – see Equation 2.1 – if the constituent concentration \bar{A} is accepted as the starting value 25–50 iteration steps are required to obtain an accuracy of 10^{-10} (g/dl) in $[A_1]$. This number can be reduced to 2–4 by initiating the iteration with a value of A_1 which approaches the final value of the root more closely. To this end we proceed as follows. The width of the boundary is increased with the length of one box at each successive transport round (see Figure 4.1). Since A_1 has the largest mobility and the complexes dissociate in the reaction boundary (GILBERT and JENKINS, 1959) the concentration of A_1 will increase in the ascending reaction boundary. We now assume that the concentration of A_1 will vary linearly over the reaction boundary (Figure 4.1). Simple geometry then yields the following expression for the starting value of the iteration procedure:

$$[A_1]_{r,n}^{\text{start}} = \frac{m-r}{m} [A_1]_{r,n-1} + \frac{r}{m} [A_1]_{r-1,n-1} \quad (4.1)$$

where n is the number of the transport round, r is box number and m is the width of the boundary after the n^{th} transport round. In the descending reaction boundary where the concentration of A_1 decreases, a similar reasoning can be applied (see Figure 4.1).

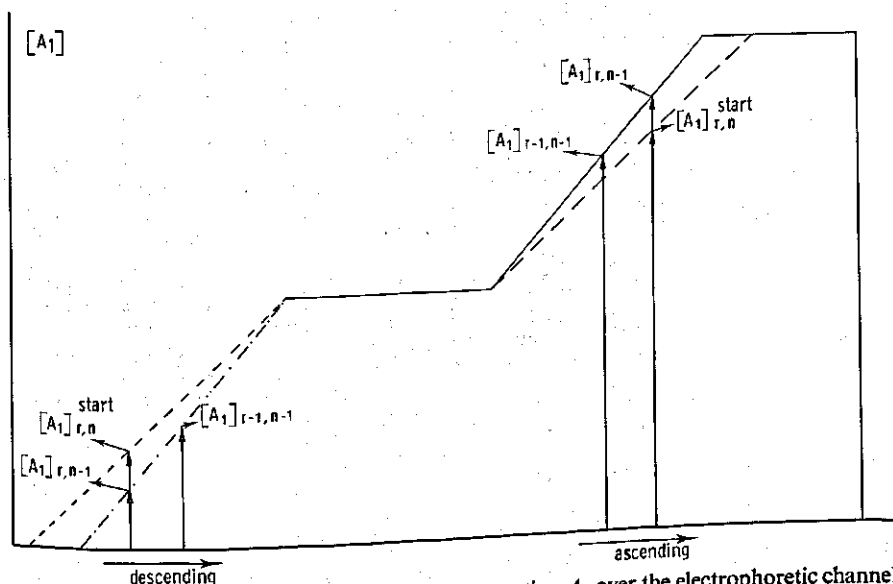


FIG. 4.1 Schematic picture of the monomer concentration A_1 over the electrophoretic channel during simulation. Ascending limb:

— boundary after $n-1$ transport rounds,
 --- boundary after n transport rounds.

Descending limb:

— boundary after $n-1$ transport rounds,
 --- boundary after n transport rounds.

In the output the concentrations of the different components over the reaction boundary are listed (see Table 4.1). Also, the velocities and the concentration gradient are given in Table 4.1. The latter is also presented as a schlieren pattern (see for instance Figure 3a-c). Furthermore the velocities of the extrema of the schlieren pattern and the area distribution under the bimodal peak are computed.

TABLE 4.1 Representing the concentrations of the various species present, the concentration gradient and the velocities over the different boxes corresponding to the schlieren pattern shown in Figure 3.3b.

NR	ALPHA	BETA	COMPLEX1	COMPLEX2	COMPLEX3	COMPLEX4	COMPLEX5
0	+0.0175	+0.3469	+0.0606	+0.0533	+0.1354	+0.2488	+0.0696
1	+0.0176	+0.3335	+0.0589	+0.0522	+0.1339	+0.2484	+0.0701
2	+0.0181	+0.3006	+0.0544	+0.0494	+0.1300	+0.2470	+0.0715
3	+0.0187	+0.2578	+0.0483	+0.0455	+0.1241	+0.2444	+0.0733
4	+0.0195	+0.2164	+0.0422	+0.0414	+0.1173	+0.2404	+0.0750
5	+0.0203	+0.1614	+0.0368	+0.0375	+0.1104	+0.2353	+0.0763
6	+0.0210	+0.1532	+0.0322	+0.0340	+0.1039	+0.2295	+0.0772
7	+0.0217	+0.1308	+0.0284	+0.0310	+0.0979	+0.2233	+0.0776
8	+0.0224	+0.1129	+0.0253	+0.0284	+0.0923	+0.2169	+0.0776
9	+0.0230	+0.0985	+0.0226	+0.0261	+0.0871	+0.2103	+0.0773
10	+0.0235	+0.0866	+0.0204	+0.0241	+0.0824	+0.2037	+0.0767
11	+0.0241	+0.0767	+0.0184	+0.0223	+0.0779	+0.1970	+0.0758
12	+0.0245	+0.0683	+0.0168	+0.0207	+0.0738	+0.1903	+0.0747
13	+0.0250	+0.0610	+0.0153	+0.0192	+0.0698	+0.1835	+0.0735
14	+0.0255	+0.0547	+0.0139	+0.0178	+0.0660	+0.1767	+0.0720
15	+0.0259	+0.0491	+0.0127	+0.0166	+0.0624	+0.1698	+0.0704
16	+0.0263	+0.0442	+0.0116	+0.0154	+0.0588	+0.1627	+0.0685
17	+0.0267	+0.0397	+0.0106	+0.0143	+0.0554	+0.1556	+0.0665
18	+0.0271	+0.0357	+0.0097	+0.0132	+0.0520	+0.1482	+0.0643
19	+0.0275	+0.0320	+0.0088	+0.0122	+0.0486	+0.1407	+0.0619
20	+0.0279	+0.0286	+0.0080	+0.0112	+0.0453	+0.1329	+0.0593
21	+0.0283	+0.0254	+0.0072	+0.0102	+0.0420	+0.1248	+0.0565
22	+0.0287	+0.0225	+0.0064	+0.0093	+0.0386	+0.1164	+0.0534
23	+0.0290	+0.0197	+0.0057	+0.0084	+0.0353	+0.1076	+0.0500
24	+0.0294	+0.0172	+0.0050	+0.0075	+0.0319	+0.0985	+0.0463
25	+0.0298	+0.0148	+0.0044	+0.0066	+0.0285	+0.0890	+0.0424
26	+0.0301	+0.0125	+0.0038	+0.0057	+0.0250	+0.0792	+0.0382
27	+0.0305	+0.0104	+0.0032	+0.0049	+0.0216	+0.0691	+0.0337
28	+0.0308	+0.0085	+0.0026	+0.0041	+0.0182	+0.0588	+0.0290
29	+0.0311	+0.0067	+0.0021	+0.0033	+0.0148	+0.0485	+0.0242
30	+0.0314	+0.0051	+0.0016	+0.0026	+0.0117	+0.0386	+0.0194
31	+0.0317	+0.0038	+0.0012	+0.0019	+0.0088	+0.0293	+0.0149
32	+0.0319	+0.0026	+0.0008	+0.0014	+0.0063	+0.0210	+0.0108
33	+0.0321	+0.0017	+0.0006	+0.0009	+0.0042	+0.0141	+0.0073
34	+0.0323	+0.0011	+0.0003	+0.0006	+0.0026	+0.0087	+0.0045
35	+0.0323	+0.0006	+0.0002	+0.0003	+0.0015	+0.0049	+0.0026
36	+0.0324	+0.0003	+0.0000	+0.0002	+0.0007	+0.0025	+0.0013
37	+0.0324	+0.0001	+0.0000	+0.0000	+0.0003	+0.0011	+0.0006
38	+0.0324	+0.0000	+0.0000	+0.0000	+0.0001	+0.0004	+0.0002
39	+0.0324	+0.0000	+0.0000	+0.0000	+0.0000	+0.0001	+0.0000
40	+0.0324	+0.0000	+0.0000	+0.0000	+0.0000	+0.0000	+0.0000

The program calculates the reaction boundary using the equilibrium constants as variable parameters. The proper set of equilibrium constants is found by trial and error. This stage of the computations can be speeded up by calculating the areas of the leading ascending and trailing descending peaks and the constituent velocities for different sets of equilibrium constants only by Equations 2.3-2.8. As will be clear from the theory presented in Chapter 2, these

COMPLEX6	POLYMER	TOTAL	DC/DR	VELOCITY	NR
+0.0369	+0.0310	+1.0000	+0.000 000	+0.000 096 000	0
+0.0375	+0.0320	+0.9842	+0.015 791	+0.000 099 391	1
+0.0392	+0.0346	+0.9447	+0.039 482	+0.000 102 783	2
+0.0416	+0.0388	+0.8926	+0.052 159	+0.000 106 174	3
+0.0443	+0.0441	+0.8407	+0.051 901	+0.000 109 565	4
+0.0469	+0.0502	+0.7951	+0.045 575	+0.000 112 957	5
+0.0492	+0.0567	+0.7569	+0.038 219	+0.000 116 348	6
+0.0511	+0.0633	+0.7251	+0.031 806	+0.000 119 739	7
+0.0526	+0.0700	+0.6983	+0.026 732	+0.000 123 130	8
+0.0538	+0.0768	+0.6755	+0.022 854	+0.000 126 522	9
+0.0547	+0.0836	+0.6556	+0.019 920	+0.000 129 913	10
+0.0552	+0.0904	+0.6379	+0.017 701	+0.000 133 304	11
+0.0556	+0.0973	+0.6218	+0.016 021	+0.000 136 696	12
+0.0557	+0.1041	+0.6071	+0.014 751	+0.000 140 087	13
+0.0556	+0.1111	+0.5933	+0.013 798	+0.000 143 478	14
+0.0552	+0.1181	+0.5802	+0.013 097	+0.000 146 870	15
+0.0547	+0.1253	+0.5676	+0.012 602	+0.000 150 261	16
+0.0539	+0.1326	+0.5553	+0.012 281	+0.000 153 652	17
+0.0529	+0.1401	+0.5432	+0.012 110	+0.000 157 043	18
+0.0516	+0.1478	+0.5311	+0.012 074	+0.000 160 435	19
+0.0501	+0.1557	+0.5190	+0.012 162	+0.000 163 826	20
+0.0484	+0.1639	+0.5066	+0.012 367	+0.000 167 217	21
+0.0463	+0.1724	+0.4939	+0.012 682	+0.000 170 609	22
+0.0440	+0.1811	+0.4808	+0.013 096	+0.000 174 000	23
+0.0413	+0.1901	+0.4672	+0.013 597	+0.000 177 391	24
+0.0382	+0.1994	+0.4531	+0.014 159	+0.000 180 783	25
+0.0349	+0.2090	+0.4383	+0.014 741	+0.000 184 174	26
+0.0311	+0.2187	+0.4230	+0.015 279	+0.000 187 565	27
+0.0271	+0.2284	+0.4074	+0.015 679	+0.000 190 957	28
+0.0228	+0.2379	+0.3915	+0.015 817	+0.000 194 348	29
+0.0185	+0.2470	+0.3760	+0.015 547	+0.000 197 739	30
+0.0143	+0.2554	+0.3613	+0.014 738	+0.000 201 130	31
+0.0104	+0.2627	+0.3479	+0.013 313	+0.000 204 522	32
+0.0071	+0.2687	+0.3366	+0.011 315	+0.000 207 913	33
+0.0044	+0.2732	+0.3277	+0.008 940	+0.000 211 304	34
+0.0025	+0.2763	+0.3212	+0.006 503	+0.000 214 696	35
+0.0013	+0.2781	+0.3168	+0.004 349	+0.000 218 087	36
+0.0006	+0.2788	+0.3141	+0.002 726	+0.000 221 478	37
+0.0002	+0.2789	+0.3124	+0.001 709	+0.000 224 870	38
+0.0000	+0.2784	+0.3112	+0.001 226	+0.000 228 261	39
+0.0000	+0.2775	+0.3100	+0.001 142	+0.000 231 652	40

quantities are indicative of the value of the equilibrium constants. The advantage of this procedure lies in the fact that only the equilibrium concentrations in the undisturbed solution are calculated, which requires a minimum of computer time.

4. 2. THE COMPUTATION PARAMETERS

The actual parameters necessary for the input of the program are presented in the following list of formal parameters. They have been placed in the order in which they are processed by the computer.

- n: number of boxes;
- A: initial concentration of A (g/dl);
- B: initial concentration of B (g/dl);
- E: electric field strength (V/cm);
- AM: molecular weight of component A ;
- BM: molecular weight of component B ;
- p: degree of polymerization (A_p);
- q: stoichiometry of complex (A_qB);
- MU: array with elements MU[1]... MU[q+3], representing the mobilities ($\text{cm}^2/\text{V.s}$) of respectively A , B , AB , A_2B , ..., A_qB and the polymers of A which have equal mobilities (see Chapter 2).
- KQ: array with elements KQ[i], where $i = 0(1)q$;
representing the complex forming constants defined as
 $KQ[i] = A_iB/A_iB$ (dl/g); note that $KQ[0] = 1$;
- KP: array with elements KP[i], where $i = 1(1)p+1$; representing the polymerization constants defined as $KP[i] = A_i/A^i$; note that $KP[1] = 1$ and $KP[p+1] = 0$.

Other actual parameters which are important corresponding to the formal parameters are:

- H: array with elements H[0]... H[p+q], representing the coefficients of the polynomial of equation 3.6;
- T: array with elements T[1]... T[p+q], representing the part of the former polynomial which is independent of \bar{A} and \bar{B} (see Equation 3.6);
- LA: array with elements LA[i], where $i = 0(1)q$,
 $LA[i] = \lambda_i = MB/(iMA + MB)$;
- LO: array with elements LO[i], where $i = 0(1)q$, $LO[i] = 1 - LA[i]$;
- C: two dimensional array C[j, i], where $j = 0(1)n$ and $i = 1(1)q+5$. The box number is represented by j, and i indicates the concentration of the q+2 solute species (A , B , AB , A_2B , ..., A_qB), polymer concentration of A , total concentration and the concentration gradient.

4.3. THE PROGRAM LISTS

```

comment ASC-PQ ASSOCIATIONSTRANSPORT H.NIJHUIS;

begin integer n,i,j,p,q,r,d,k,vo,vi,m,s;
      real c1,c2,c3,c4,c5,a,b,x,y,diff,eps,tol,w,wa,AM,BM,E,
           vb,ve,su,xm,uw,vm,hp,cor;
      boolean good,stylg;
      array H,MA[0:20],T,KP,MU,KC,LA,LØ,LK,KQ,KR[0:10];
AAA:  INPUT(60,t1,n,a,b,E,AM,BM,p,q,eps); good:=true;
      for j:=1 step 1 until q+3 do INPUT(60,t1,MU[j]);
      for j:=0 step 1 until q do INPUT(60,t1,KQ[j]);
      for j:=1 step 1 until p+1 do INPUT(60,t1,KP[j]);
      if KQ[0] #1 then good:=false;
      if KP[1] #1 then good:=false;
      if KP[p+1]#0 then good:=false;
      if good=false then goto SØS;
      KC[0]:=KQ[0]; s:=p; if s < q then s:=q;
      for j:=1 step 1 until q do KC[j]:=KQ[j]×KP[j];
      for j:=2 step 1 until p+1 do KR[j]:=KP[j]/KP[j-1];
      diff:=1/(EX(MU[1]-MU[2]));
      for j:=1 step 1 until q+3 do MU[j]:=diff×MU[j]×E;
      for j:=1,3 step 1 until q+3 do MU[j]:=MU[j]-MU[2];
      vo:=vi:=0; cor:=0; r:=p+q; d:=r-1;
      for j:=0 step 1 until q do LA[j]:=BM/(BM+j×AM);
      for j:=0 step 1 until q do LØ[j]:=1-LA[j];
      for j:=0 step 1 until q do LK[j]:=LA[j]×KC[j];
      for j:=0 step 1 until r do H[j]:=0;
      for i:=1 step 1 until p do
      for j:=0 step 1 until q do H[i+j]:=H[i+j]+LK[j]×KP[i];
      for j:=1 step 1 until q do T[j]:=H[j];
      tol:=0.0001/n/n; hp:=H[r]; MA[0]:=T;

begin array c[1:q+5,0:n];

real procedure NERA(x); real x;
begin w:=wa:=hp; k:=d;
SSS: w:=w×x+H[k]; wa:=w×x+w; k:=k-1;
      if k>0 then goto SSS; NERA:=(w×x+H[k])/wa;
end procedure NERA;

```

```

real procedure REEQ(i); integer i;
begin  y:=c[1,1]-cor; c1:=c2:=c4:=c5:=0;
      for j:=1 step 1 until q do c1:=c1+L0[j]*c[j+2,1];
      for j:=0 step 1 until q do c2:=c2+LA[j]*c[j+2,1];
      c1:=c1+c[1,1]+c[q+3,1]; c3:=c1+c2;
      for j:=0 step 1 until q do H[j]:=T[j]+c2*KC[j]-c3*LK[j];
CYC:   x:=y; y:=x-NEEA(x); if tol<abs(x-y) then goto CYC;
      for j:=1 step 1 until s do MA[j]:=y*MA[j-1];
      for j:=0 step 1 until q do c5:=c5+LK[j]*MA[j];
      c[1,1]:=y; c[2,1]:=c2:=c2/c5;
      for j:=1 step 1 until q do c[j+2,1]:=KC[j]*MA[j]*c2;
      for j:=2 step 1 until p do c4:=c4+KP[j]*MA[j]; c[q+3,1]:=c4
end procedure REEQ;

      for i:=0 step 1 until n do
      for j:=1 step 1 until q+5 do c[j,1]:=0;
      c[1,0]:=a; c[2,0]:=b; REEQ(0); c[q+4,0]:=a+b;

HHH:   vi:=vi+1; m:=0;
      for i:=n step -1 until 1 do
      begin if c[1,i-1]<tol then goto VVV;
      for j:=q+3 step -1 until 3,1 do
      begin cor:=c[j,(i-1)]-c[j,i];
      c[j,i]:=c[j,i]+cor*MU[j] end;
      if m=0 then m:=i; cor:=cor*(m-1)/m; REEQ(i);
VVV:   end transport;

su:=0; for j:=1 step 1 until q+3 do
su:=su+c[j,0]-c[j,1];
if abs(su)<eps then
begin
for i:=1 step 1 until n-1 do
for j:=1 step 1 until q+3 do c[j,i]:=c[j,i+1];
vo:=vo+1; goto HHH
end moving frame;

```

```

su:=0; for j:=3 step 1 until q+2 do su:=su+c[j,n];
if su<eps then goto HHH;

for i:=1 step 1 until n do
  begin for j:=1 step 1 until q+3 do
    c[q+4,i]:=c[q+4,i] + c[j,i];
    c[q+5,i]:=c[q+4,i-1]-c[q+4,i] end;
vb:=(MU[2]+vo/vi)/diff; diff:=diffxvi; k:=0; ve:=n/diff+vb;
for i:=0 step 1 until n do
  begin if i=0 v i-kx50=1 then
    begin k:=k+1;
    OUTPUT(61,{x/97b{page},bzd},k);
    OUTPUT(61,{/ b{nr alpha beta }});
    for j:=1 step 1 until q do
      OUTPUT(61,{complex}d1b},j);
      OUTPUT(61,{b{polymer total dc/dr}});
      OUTPUT(61,{7b{velocity nr}});
    if k>1 then OUTPUT(61,{/});
    end;
    OUTPUT(61,{/2zd2b},i);
    for j:=1 step 1 until q+4 do
      OUTPUT(61,{+zd.4d1b},c[j,i]);
      OUTPUT(61,{+zd.3db3d1b},c[q+5,i]);
      OUTPUT(61,{+zd.3db3db3d,b2zd},i/diff+vb,i);
    if i:10=i/10 then OUTPUT(61,{/});
    end result one box;

if 25<n then OUTPUT(61,{x}) else OUTPUT(61,{/});
for i:=1 step 1 until n do
  begin
    OUTPUT(61,{/zzd3b},i); m:=c[q+5,i]x1000xnxn/625;
    if m>129 then k:=0 else k:=i;
    if k=0 then m:=128;
    for j:=1 step 1 until m do OUTPUT(61,{x});
    if k=0 then OUTPUT(61,{o});
  end graph;

```

```

OUTPUT(61,{x 97b{page},zd,0});
OUTPUT(61,{/9b{ASC-PQ ASSOCIATIONTRANSPORT H.NIJHUIS}});
OUTPUT(61,{5b{ascending reaction boundary}});
OUTPUT(61,{/ 9b{alpha- en beta-casein }});
OUTPUT(61,{ 2b{alpha-cas. polymerizing }});
OUTPUT(61,{ 2b{alpha en beta complexes: a/b=q/1 }});
OUTPUT(61,{// 9b{boxes amount}21b2zd },n);
OUTPUT(61,{ 14b{field strength (volt/cm) }8bzd.4d },E );
OUTPUT(61,{/ 9b{initial conc. alpha (g/dl)} 8bzd.4d },a);
OUTPUT(61,{ 9b{mol weight alpha-cas. } 7b5zd },AM);
OUTPUT(61,{/ 9b{initial conc. beta (g/dl)} 9bzd.4d },b);
OUTPUT(61,{ 9b{mol weight beta-cas. } 8b5zd },BM);
OUTPUT(61,{/ 9b{delta T/delta x (sec/cm) } 5b5zd },diff/v1);
OUTPUT(61,{ 14b{accuracy in conc. (g/dl)}10bd.7d },eps);
OUTPUT(61,{// 9b{ass.const. KC(i)=c(i)/bx(a)i (dl/g)i }});
OUTPUT(61,{4b{KQ[i]=c1/bxa1 (dl/g) }});
OUTPUT(61,{4b{KA[i]=c1/axo(i-1) (dl/g) }});
OUTPUT(61,{/20b,zd,5bd.5d$+3d},0,KC[0] );
for i:=1 step 1 until q do
  begin
    OUTPUT(61,{/20b,zd,5bd.5d$+3d},i,KC[i] );
    OUTPUT(61,{13b2zd.d,23b2zd.d},KQ[i];KC[i]/KC[i-1]);
  end;

OUTPUT(61,{// 9b{mobilities}});
for j:=1,3 step 1 until q+3 do MU[j]:=MU[j]+MU[2];
for j:=1 step 1 until q+3 do MU[j]:=MU[j]xv1/(Exdiff);
OUTPUT(61,{/ 9b{alpha (cm2/voltxsec)} },MU[1]);
OUTPUT(61,{/ 9b{beta (cm2/voltxsec)} },MU[2]);
for j:=1 step 1 until q do
  OUTPUT(61,{/ 9b{complex}d,{(cm2/voltxsec)} },j,MU[j+2]);
  OUTPUT(61,{/ 9b{polymer (cm2/voltxsec)} },MU[q+3]);
  OUTPUT(61,{// 9b{polymerization-cons. KP=ap/(a1)p }});
  OUTPUT(61,{4b{KR=a(p)/a(p-1)xa (dl/g) }});
  OUTPUT(61,{ 4b{polymerization degree alpha }2zd },p);
  OUTPUT(61,{/20b,zd,5bd.5d$+3d},1,KP[1] );
  for i:=2 step 1 until p+1 do
    OUTPUT(61,{/20b,zd,5bd.5d$+3d,11b2zd.d},i,KP[i],KR[i] );

```

```

OUTPUT(61,{2/11b{transport rounds executed }3b6zd{,v1};
OUTPUT(61,{ 11b{moving frame rounds executed }6zd{,vo);

OUTPUT(61,{20b{velocities (cm/sec)}1});
OUTPUT(61,{ 11b{box nr 0}+3zd.3db3db3d{,vb);
OUTPUT(61,{ 11b{box nr}2zd,+3zd.3db3db3d{,n,ve);
OUTPUT(61,{ 11b{difference}+2zd.3db3db3d{,ve-vb);

OUTPUT(61,{4/13b{maxima and minima in gradient }1});
OUTPUT(61,{4/11b{box}12b{velocity}9b{area}});
  c2:=c[q+5,0]; c3:=c[q+5,1]; c5:=c[q+4,0];
  if c2<c3 then styg:=true else styg:=false;
  for i:=2 step 1 until n do
  begin
    c1:=c2; c2:=c3; c3:=c[q+5,1]; c4:=c5;
    if c2<c3 = styg then goto OUT;
    if styg=true then styg:=false else styg:=true;
    uw:=(c1-c3)/(c1+c3-2xc2)/2; xm:=1-1+uw; vm:=xm/diff+vb;
    if uw>0 then k:=1 else k:=-1;
    c5:=c[q+4,i-1]-kxuwxc[q+4,i-1]-c[q+4,i+k-1]; su:=c4-c5;
    OUTPUT(61,{4/8b3z2d.3d,4b+zd.3db3db3d,5b+zd.4d{,xm,vm,su);
  OUT:  end;
    OUTPUT(61,{4/41b+zd.4d{,c5-c[q+4,n]});

c1:=MU[1]x(c[1,0]+c[q+3,0]); c2:=0;
for j:=3 step 1 until q+2 do c1:=c1+L0[j-2]xc[j,0]xMU[j];
for j:=2 step 1 until q+2 do c2:=c2+LA[j-2]xc[j,0]xMU[j];
c1:=c1/a; c2:=c2/b; su:=ax(c1-c2)/(MU[1]-c2);
OUTPUT(61,{ 13b{area leading peak}});
OUTPUT(61,{4/12b{obs}7b{per}6b{cal}7b{per}});
OUTPUT(61,{4/10b+zd.4d3b,+zd.d{,c[q+4,n],c[q+4,n]x100/(a+b));
OUTPUT(61,{4+3bzd.4d3b,+zd.d{,su,sux100/(a+b));
OUTPUT(61,{4/3b{const.velocity alpha}4b+zd.3db3db3d{,c1);
OUTPUT(61,{4/3b{const.velocity beta}5b+zd.3db3db3d{,c2);

  if KP[1]=1 ^ KP[p+1]=0 then goto AAA
end;
SOS:  if good=false then OUTPUT(61,{mistake});
end

```

comment DESC-PQ ASSOCIATIONSTRANSPORT H.NIJHUIS;

```

begin integer n,i,j,p,q,r,d,k,vo,vi,m,s;
real c1,c2,c3,c4,c5,a,b,x,y,diff,eps,tol,w,wa,AM,BM,E,
vb,ve,su,xm,uw,vn,hp,cor,mu1,mu2,mud;
boolean good,glyk,sty;
array H,MA[0:20],T,KP,MU,KC,LA,LØ,LK,KQ,KR[0:10];
AAA: INPUT(60,t),n,a,b,E,AM,BM,p,q,eps); good:=glyk:=true;
if n<0 then goto SØS;
for j:=1 step 1 until q+3 do INPUT(60,t),MU[j]);
for j:=0 step 1 until q do INPUT(60,t),KQ[j]);
for j:=1 step 1 until p+1 do INPUT(60,t),KP[j]);
if KQ[0] #1 then good:=false;
if KP[1] #1 then good:=false;
if KP[p+1]#0 then good:=false;
if good=false then goto SØS;
KC[0]:=KQ[0]; s:=p; if s < q then s:=q;
for j:=1 step 1 until q do KC[j]:=KQ[j]×KP[j];
for j:=2 step 1 until p+1 do KR[j]:=KP[j]/KP[j-1];
diff:=1/(EX(MU[1]-MU[2])); vo:=vi:=0; cor:=0;
for j:=1 step 1 until q+3 do MU[j]:=diff×MU[j]×E;
mu1:=MU[1]; mu2:=MU[2]; mud:=mu1-mu2; r:=p+q; d:=r-1;
for j:=1 step 1 until q+3 do MU[j]:=MU[j]-mu2;
for j:=1 step 1 until q+3 do MØ[j]:=mud-MU[j];
for j:=0 step 1 until q do LA[j]:=BM/(BM+j×AM);
for j:=0 step 1 until q do LØ[j]:=1-LA[j];
for j:=0 step 1 until q do LK[j]:=LA[j]×KC[j];
for j:=0 step 1 until r do H[j]:=0;
for i:=1 step 1 until p do
for j:=0 step 1 until q do H[i+j]:=H[i+j]+LK[j]×KP[i];
for j:=0 step 1 until q do T[j]:=H[j];
tol:=0.0001/n/n; hp:=H[r]; MA[0]:=t;

begin array c[1:q+5,0:n];

real procedure NERA(x); real x;
begin w:=wa:=hp; k:=d;
SSS: w:=w×x+H[k]; wa:=w×x+w; k:=k-1;
if k>0 then goto SSS; NERA:=(w×x+H[k])/wa;
end procedure NERA;

```

```

real procedure REEQ(i); integer i;
begin  y:=c[1,i]-cor; c1:=c2:=c4:=c5:=0;
      for j:=1 step 1 until q do c1:=c1+L0[j]*c[j+2,i];
      for j:=0 step 1 until q do c2:=c2+LA[j]*c[j+2,i];
      c1:=c1+c[1,i]+c[q+3,i]; c3:=c1+c2;
      for j:=0 step 1 until q do H[j]:=T[j]+c2*KC[j]-c3*LK[j];
CYC:   x:=y; y:=x-NEEA(x); if tol<abs(x-y) then goto CYC;
      for j:=1 step 1 until s do MA[j]:=y*MA[j-1];
      for j:=0 step 1 until q do c5:=c5+LK[j]*MA[j];
      c[1,i]:=y; c[2,i]:=c2:=c2/c5;
      for j:=1 step 1 until q do c[j+2,i]:=KC[j]*MA[j]*c2;
      for j:=2 step 1 until p do c4:=c4+KP[j]*MA[j]; c[q+3,i]:=c4
end procedure REEQ;

      for i:=0 step 1 until n do
      for j:=1 step 1 until q+5 do c[j,i]:=0;
      c[1,0]:=a; c[2,0]:=b; REEQ(0); c[q+4,0]:=a+b;

HHH:   vi:=vi+1; m:=0; glyk:=true;
      for i:=n step -1 until 1 do
        begin if c[1,i-1]<tol then goto VVV;
              for j:=q+3 step -1 until 1 do
                begin cor:=c[j,(i-1)]-c[j,i];
                  c[j,i]:=c[j,i]+cor*XMU[j] end;
                if m=0 then m:=i; cor:=cor*(m-1)/m; REEQ(i);
VVV:   end transport;

      for j:=1 step 1 until q+2 do
      if abs(c[j,0]-c[j,1]) > eps then glyk:=false;
      if glyk = true then
        begin
          for i:=1 step 1 until n-1 do
          for j:=1 step 1 until q+3 do c[j,i]:=c[j,i+1];
          vo:=vo+1; goto HHH
        end moving frame;

```

```

su:=0; for j:=3 step 1 until q+2 do su:=su+c[j,n];
if su<eps then goto HHH;

for i:=1 step 1 until n do
  begin for j:=1 step 1 until q+3 do
    c[q+4,i]:=c[q+4,i] + c[j,i];
    c[q+5,i]:=c[q+4,i-1]-c[q+4,i] end;
  vb:=(mul-vo/vi)/diff; diff:=-diff*vi; k:=0; ve:=n/diff+vb;
  for i:=0 step 1 until n do
    begin if i=0 v i-k<50=1 then
      begin k:=k+1;
        OUTPUT(61,{x/97b{page},bzd},k);
        OUTPUT(61,{ / b{nr} alpha beta });
        for j:=1 step 1 until q do
          OUTPUT(61,{complex{d1b}},j);
          OUTPUT(61,{b{polymer} total dc/dr});
          OUTPUT(61,{7b{velocity} nr}/);
          if k>1 then OUTPUT(61,{//});
        end;
        OUTPUT(61,{/2zd2b},i);
        for j:=1 step 1 until q+4 do
          OUTPUT(61,{zd.4d1b},c[j,i]);
          OUTPUT(61,{zd.3db3d1b},c[q+5,i]);
          OUTPUT(61,{zd.3db3db3d,b2zd},i/diff+vb,i);
        if i:10=i/10 then OUTPUT(61,{/});
        end result one box;

      if 25<n then OUTPUT(61,{x}) else OUTPUT(61,{//});
      for i:=n step -1 until 1 do
        begin
          OUTPUT(61,{/zzd3b},i); m:=c[q+5,i]*1000*xn*xn/625;
          if m>129 then k:=0 else k:=I;
          if k=0 then m:=128;
          for j:=1 step 1 until m do OUTPUT(61,{x});
          if k=0 then OUTPUT(61,{o});
        end graph;

```



```

OUTPUT(61,{x 97b{page},zd},0);
OUTPUT(61,{/9b{DESC-PQ ASSOCIATIONTRANSPORT H.NIJHUIS}});
OUTPUT(61,{5b{descending reaction boundary}});
OUTPUT(61,{/ 9b{alpha- en beta-casein }});
OUTPUT(61,{ 2b{alpha-cas. polymerizing }});
OUTPUT(61,{ 2b{alpha and beta complexes: a/b=q/1 }});
OUTPUT(61,{// 9b{boxes amount}21b2zd },n);
OUTPUT(61,{ 14b{field strength (volt/cm) }8bzd.4d},E );
OUTPUT(61,{/ 9b{initial conc. alpha (g/dl)}8bzd.4d },a);
OUTPUT(61,{ 9b{mol weight alpha-cas. }7b5zd},AM);
OUTPUT(61,{/ 9b{initial conc. beta (g/dl)}9bzd.4d },b);
OUTPUT(61,{ 9b{mol weight beta-cas. }8b5zd},BM);
OUTPUT(61,{/ 9b{delta T/delta x (sec/cm) }5b5zd },-diff/vi);
OUTPUT(61,{ 14b{accuracy in conc. (g/dl)}10bd.7d},eps);
OUTPUT(61,{// 9b{ass.const. KC(1)=c(i)/bx(a)1 (dl/g)1 }});
OUTPUT(61,{4b{KQ[1]=ci/bxai (dl/g) }});
OUTPUT(61,{4b{KA[1]=ci/axc(i-1) (dl/g) }});
OUTPUT(61,{/20b,zd,5bd.5d$+3d},0,KC[0] );
for i:=1 step 1 until q do
  begin
    OUTPUT(61,{/20b,zd,5bd.5d$+3d},i,KC[1] );
    OUTPUT(61,{13b2zd.d,23b2zd.d},KQ[1];KC[1]/KC[i-1])
  end;

OUTPUT(61,{// 9b{mobilities}});
for j:=1 step 1 until q+3 do MU[j]:=-MU[j]+mud;
for j:=1 step 1 until q+3 do MU[j]:=MU[j]+mu2;
for j:=1 step 1 until q+3 do MU[j]:=-MU[j]xvi/E/diff;
OUTPUT(61,{/ 9b{alpha (cm2/voltxsec)}},MU[1]);
OUTPUT(61,{/ 9b{beta (cm2/voltxsec)}},MU[2]);
for j:=1 step 1 until q do
  OUTPUT(61,{/ 9b{complex}d,{(cm2/voltxsec)}},j,MU[j+2]);
  OUTPUT(61,{/ 9b{polymer (cm2/voltxsec)}},MU[q+3]);
  OUTPUT(61,{// 9b{polymerization-cons. KP=ap/(a1)p }});
  OUTPUT(61,{4b{KR=a(p)/a(p-1)xa (dl/g) }});
  OUTPUT(61,{ 4b{polymerization degree alpha }2zd},p);
  OUTPUT(61,{/20b,zd,5bd.5d$+3d},i,KP[1] );
  for i:=2 step 1 until p+1 do
    OUTPUT(61,{/20b,zd,5bd.5d$+3d,11b2zd.d},i,KP[i],KR[i] );

```

```

OUTPUT(61,t/11b{transport rounds executed }3b6zd{,v1};
OUTPUT(61,t /11b{moving frame rounds executed }6zd{,vo};
OUTPUT(61,t//20b{velocities (cm/sec)}1});
OUTPUT(61,t /11b{box nr }0{+3zd.3db3db3d{,vb};
OUTPUT(61,t /11b{box nr}2zd,+3zd.3db3db3d{,n,ve};
OUTPUT(61,t /11b{difference}+2zd.3db3db3d{,ve-vb};

OUTPUT(61,t//13b{maxima and minima in gradient }1});
OUTPUT(61,t/11b{box}12b{velocity}9b{area}1});
c2:=c[q+5,0]; c3:=c[q+5,1]; c5:=c[q+4,0];
if c2<c3 then styg:=true else styg:=false;
for i:=2 step 1 until n do
begin
c1:=c2; c2:=c3; c3:=c[q+5,1]; c4:=c5;
if c2<c3 = styg then goto OUT;
if styg=true then styg:=false else styg:=true;
uw:=(c1-c3)/(c1+c3-2xc2)/2; xm:=i-1+uw; vm:=xm/diff+vb;
if uw>0 then k:=1 else k:=-1;
c5:=c[q+4,1-1]-kxuwx(c[q+4,1-1]-c[q+4,i+k-1]); su:=c4-c5;
OUTPUT(61,t/8b3z2d.3d,4b+zd.3db3db3d,5b+zd.4d{,xm,vm,su);
OUT: end;
OUTPUT(61,t/41b+zd.4d{,c5-c[q+4,n]);

c1:=MU[1]x(c[1,0]+c[q+3,0]); c2:=0;
for j:=3 step 1 until q+2 do c1:=c1+L0[j-2]xc[j,0]xMU[j];
for j:=2 step 1 until q+2 do c2:=c2+LA[j-2]xc[j,0]xMU[j];
c1:=c1/a; c2:=c2/b; su:=bx(c1-c2)/(c1-MU[2]);
OUTPUT(61,t /13b{area trailing peak}1});
OUTPUT(61,t/12b{obs}7b{per}6b{cal}7b{per}1});
OUTPUT(61,t/10b+zd.4d3b,+zd.d{,c[q+4,n],c[q+4,n]x100/(a+b));
OUTPUT(61,t+3bzd.4d3b,+zd.d{,su,sux100/(a+b));
OUTPUT(61,t//3b{const.velocity alpha}4b+zd.3db3db3d{,c1};
OUTPUT(61,t/3b{const.velocity beta}5b+zd.3db3db3d{,c2};

if KP[1]=1 ^ KP[p+1]=0 then goto AAA
end;
SOS: if good=false then OUTPUT(61,t{mistake});
end

```

SUMMARY

The anomalous boundaries occurring during free electrophoresis or ultracentrifugation of interacting biopolymers are investigated. As is already known from the early studies of LONGSWORTH and MACINNES (1942), such interactions can give rise to abnormal velocities and areas of the migrating peaks in transport patterns.

In this thesis in particular the complex formation between α_{s1} - and β -casein two major proteins from milk, was studied. The importance of such complex formation for the cohesion of the natural casein micelles in milk has been stressed repeatedly.

Complex formation between these proteins was easily recognizable from the different number of moving peaks on both sides of the electrophoretic channel.

Application of the moving boundary theory (Chapter 2) leads to the conclusion that the constituent mobility of α_{s1} -casein is fairly high, which indicates the presence of complexes of a high stoichiometric ratio α_{s1}/β .

The development of the reaction boundaries during electrophoresis was simulated in the ALGOL-programs presented in Chapter IV. In the computations the self-polymerization of α_{s1} -casein under the experimental conditions and the simultaneous formation of the various complexes was taken into account. The results of such a simulation was found to be consistent with the conclusions of the moving boundary theory.

The simulation (Chapter 3) is brought about by dividing the electrophoretic channel into a large number of small boxes of equal length. The development of the reaction boundary then was simulated by means of alternate rounds of transport of material from one box to the next and subsequent re-equilibration. Only the transport due to the velocity is accounted for, which makes the procedure a simplification of GOAD's method for the numerical solution of the conservation-of-mass equation of a system of migrating and interacting macromolecules. By reducing the calculation in this way a diffusion-like error is introduced which is used to advantage to imitate the diffusional flux. It is shown that this procedure is essentially identical to the countercurrent analog developed by BETHUNE and KEGELES to account for the effect of diffusion on the transport pattern of interacting proteins.

The adjustment of the simulated diffusion coefficients to their actual values is discussed and the results of different calculations compared. It is shown that in agreement with expectation diffusional spreading had only a minor influence on the development of a reaction boundary in prolonged experiments.

SAMENVATTING

Onderzocht werden de anomalieën in de bewegende grenzen, die optreden tijdens vrije elektroforese of ultracentrifugering van biopolymeren waartussen interacties bestaan. Uit de studies van LONGSWORTH en MACINNES in 1942 was reeds bekend dat zulke interacties aanleiding kunnen geven tot abnormale snelheden en oppervlakken van de zich verplaatsende pieken in transportexperimenten.

In dit proefschrift wordt de complexvorming bestudeerd tussen twee hoofdcomponenten van de melkeiwitten, namelijk α_{s1} - en β -caseïne. Op het belang van deze complexvorming voor de stabiliteit van caseïnemicellen is herhaaldelijk de nadruk gelegd.

De complexvorming tussen deze twee eiwitten was gemakkelijk herkenbaar aan het verschillende aantal pieken dat optreedt in de beide benen van het U-vormige elektroforesekanaal.

Door de 'moving boundary'-theorie (hoofdstuk 2) toe te passen, kan worden geconcludeerd dat de constituentsnelheden van α_{s1} -caseïne tamelijk hoog zijn, wat een aanwijzing is voor de aanwezigheid van complexen met een hoge stoichiometrische verhouding α_{s1}/β .

De ontwikkeling van de reactie-grenzen tijdens elektroforese is gesimuleerd in de ALGOL-programma's die in hoofdstuk 4 gegeven zijn. In de simulatie wordt rekening gehouden met de polymerisatie van α_{s1} -caseïne onder de experimentele omstandigheden en de gelijktijdige vorming van de verschillende complexen. Het resultaat van deze berekening bleek overeen te stemmen met dat van de 'moving boundary'-theorie.

In de simulatie (hoofdstuk 3) wordt het elektroforesekanaal in een groot aantal hokjes van gelijke diepte verdeeld. De vorming van de reactie-boundary wordt dan gesimuleerd door afwisselend de componenten van het ene naar het andere hokje te transporteren en daarna in de aldus ontstane inhoud van de hokjes het chemisch evenwicht zich opnieuw te laten instellen. Alleen het massa-transport ten gevolge van het van buiten aangebrachte potentiaalveld wordt in rekening gebracht.

De gebruikte methode is zodoende een vereenvoudiging van de methode van GOAD voor het numeriek oplossen van de conserveringsvergelijking van een systeem van transporterende componenten waartussen interacties bestaan. Door deze vereenvoudiging wordt er een diffusieachtige fout geïntroduceerd die ten nutte wordt aangewend om de diffusie te imiteren. Aangetoond wordt dat deze procedure in wezen vergelijkbaar is met de countercurrent-analogie waarmee BETHUNE en KEGELES de diffusie verdisconteerden in het transport van associërende eiwitten.

Het aanpassen van de gesimuleerde diffusiecoëfficiënten aan de werkelijke waarden wordt besproken en de resultaten van de verschillende berekeningen zijn vergeleken. Aangetoond wordt dat, overeenkomstig de verwachting, de spreiding ten gevolge van de diffusie slechts een ondergeschikte rol speelt in de ontwikkeling van de reactie-boundaries in langdurige experimenten.

REFERENCES

- ACKERS, G. K. and THOMPSON, T. E., *Proc. Natl. Acad. Sci. U.S.*, **53**, (1965) 342.
 ACKERS, G. K., *J. Biol. Chem.*, **242**, (1967) 3026.
 ACKERS, G. K., *Adv. Prot. Chem.*, **24**, (1970) 343.
 BALDWIN, R. L., *Biochem. J.*, **65**, (1957) 503.
 BETHUNE, J. L. and KEGELES, G., *J. Phys. Chem.*, **65**, (1961A) 433.
 BETHUNE, J. L. and KEGELES, G., *J. Phys. Chem.*, **65**, (1961B) 1755.
 BETHUNE, J. L. and KEGELES, G., *J. Phys. Chem.*, **65**, (1961C) 1761.
 BETHUNE, J. L., *J. Phys. Chem.*, **74**, (1970) 3837.
 BUCHHEIM, W. and WELSCH, U., *Neth. Milk Dairy J.*, **27**, (1973) 163.
 BUTLER, P. J. G. and KLUG, A., *Proc. Natl. Acad. Sci. U.S.*, **69**, (1972) 2950.
 CANN, J. R. and KLAPPER, J. A., *J. Biol. Chem.*, **236**, (1961) 2446.
 CANN, J. R. and GOAD, W. B., *J. Biol. Chem.*, **240**, (1965A) 148.
 CANN, J. R. and GOAD, W. B., *J. Biol. Chem.*, **240**, (1965B) 1162.
 CANN, J. R. and GOAD, W. B., *Interacting Macromolecules*, Acad. Press, New York, (1970).
 CHUN, P. W. L., *Characterization of Interacting Casein Molecules*, Thesis, University Microfilms, Inc. Ann Arbor, Michigan (1965).
 COX, D. J., *Arch. Biochem. Biophys.*, **112**, (1965A) 249.
 COX, D. J., *Arch. Biochem. Biophys.*, **112**, (1965B) 259.
 COX, D. J., *Arch. Biochem. Biophys.*, **119**, (1967) 230.
 COX, D. J., *Arch. Biochem. Biophys.*, **129**, (1969) 106.
 COX, D. J., *Arch. Biochem. Biophys.*, **142**, (1971A) 514.
 COX, D. J., *Arch. Biochem. Biophys.*, **146**, (1971B) 181.
 CRAIG, L. C. and CRAIG, D., in *Technique of Organic Chemistry* (Weissberger, A.) Interscience Publishers, Inc., New York, Vol. III (1950) 171.
 CRANK, J., *The Mathematics of Diffusion*, Clarendon Press, Oxford, 1967.
 DURHAM, A. C. H., FINCH, J. T. and KLUG, A., *Nature New Biol.*, **229**, (1971) 37.
 ELIAS, H. G., *Méthodes de l'Ultracentrifugation Analytique*, 3rd ed., Beckman Instruments International, S.A. (1964).
 FUJITA, H., *Mathematical theory of sedimentation analysis*, Acad. Press, New York (1962) 194.
 GILBERT, G. A., *Proc. Royal Soc. Ser. A.*, **250**, (1959) 377.
 GILBERT, G. A. and JENKINS, R.C.Ll., *Proc. Roy. Soc. London, Series A*, **253**, (1959) 420.
 HENN, S. W. and ACKERS, G. K., *Biochemistry*, **8**, (1969) 3829.
 HERSKOVITS, T. T., *Biochemistry*, **5**, (1966) 1018.
 VON HIPPEL, P. H. and WAUGH, D. F., *J. Am. Chem. Soc.*, **77**, (1955) 4311.
 JENNESS, R., in *Milk Proteins* (MACKENZIE, H. A.), Acad. Press, New York, Vol. 1, (1970) 17.
 KLOTZ, I. M., *Science*, **155**, (1967) 697.
 KNOOP, A. M., KNOOP, E. and WIECHEN, A., *Neth. Milk Dairy J.*, **27**, (1973) 121.
 KREJCI, L. E., JENNINGS, R. K. and DE SPAIN SMITH, L., *J. Franklin Inst.*, **232**, (1941) 592.
 KREJCI, L. E., *J. Franklin Inst.*, **234**, (1942) 197.
 LINDERSTRÖM LANG, K., *C. R. Trav. Lab. Carlsberg*, **17**, (9) (1929) 1.
 LONGSWORTH, L. G., *Chem. Rev.*, **30**, (1942) 323.
 LONGSWORTH, L. G. and MACINNES, D. A., *J. Gen. Physiol.*, **25**, (1942) 507.
 LONGSWORTH, L. G., in *Electrophoresis* (Bier, M.), Acad. Press, New York, Vol. 1, (1959) 91.
 MACKINLAY, A. G. and WAKE, R. G., in *Milk Proteins* (MACKENZIE, H. A.), Acad. Press, New York, Vol. 2, (1971) 175.
 MARGENAU, H. and MURPHY, G. M., *The Mathematics of Physics and Chemistry*, D. van Nostrand Company, Inc., New York, 15th ed., (1955) 475.
 NAUR, P., BACKUS, J. W., BAUER, F. L., GREEN, J., KATZ, C., MACCARTHY, J., PERLIS, A. J., RUTISHAUSER, H., SAMELSON, K., VAUQUOIS, B., WEGSTEIN, J. H., VAN WIJNGAARDEN, A. and WOODGER, M., *Communications of the ACM*, **6**, (1963) 1.

- NICHOL, L. W., BETHUNE, J. L., KEGELES, G. and HESS, E. L. in *The Proteins* (Neurath, H.), Acad. Press, New York, 2nd ed., Vol. 2, (1964) 305.
- NICHOL, L. W. and WINZOR, D. J., *J. Phys. Chem.*, **68**, (1964) 2455.
- NIJHUIS, H. and PAYENS, T. A. J., *Abstr. Commun. Meet. Fed. Eur. Biochem. Soc.*, **8**, (1972) 1147.
- NOELKEN, M. and REIBSTEIN, M., *Arch. Biochem. Biophys.*, **123**, (1968) 397.
- PAYENS, T. A. J. and VAN MARKWIJK, B. W., *Biochim. Biophys. Acta*, **71**, (1963) 517.
- PAYENS, T. A. J., *J. Dairy Sci.*, **49**, (1966) 1317.
- PAYENS, T. A. J. and SCHMIDT, D. G., *Arch. Biochem. Biophys.*, **115**, (1966) 136.
- PAYENS, T. A. J., *Biochem. J.*, **108**, (1968) 14P.
- PAYENS, T. A. J., BRINKHUIS, J. A. and VAN MARKWIJK, B. W., *Biochim. Biophys. Acta*, **175**, (1969) 434.
- RAO, M. S. N. and KEGELES, G., *J. Am. Chem. Soc.*, **80**, (1958) 5724.
- REITHEL, F. J., *Adv. Protein Chem.*, **18**, (1963) 123.
- SCHACHMAN, H. K., *Ultracentrifugation in Biochemistry*, Acad. Press, (1959).
- SCHMIDT, D. G. and PAYENS, T. A. J., *Biochim. Biophys. Acta*, **78**, (1963) 492.
- SCHMIDT, D. G., PAYENS, T. A. J., VAN MARKWIJK, B. W. and BRINKHUIS, J. A., *Biochem. Biophys. Res. Commun.*, **27**, (1967) 448.
- SCHMIDT, D. G., On the Association of α_{s1} -Casein, Thesis, University of Utrecht, 1969, H. Veenman & Zonen N.V., Wageningen.
- SCHMIDT, D. G., *Biochim. Biophys. Acta*, **207**, (1970) 130.
- SCHMIDT, D. G. and BUCHHEIM, W., *Milchwissenschaft*, **25**, (1970) 596.
- SCHMIDT, D. G. and PAYENS, T. A. J., *J. Coll. Interf. Sci.*, **39**, (1972) 655.
- SCHMIDT, D. G., WALSTRA, P., BUCHHEIM, W., *Neth. Milk Dairy J.*, **27**, (1973) 128.
- SINGER, S. J. and CAMBELL, D. H., *J. Am. Chem. Soc.*, **77**, (1955) 3499.
- STEINER, R. F., *Arch. Biochem. Biophys.*, **49**, (1954) 400.
- STEINER, R. F., *Biopolymers*, **9**, (1970A) 1465.
- STEINER, R. F., *Biochemistry*, **9**, (1970B) 4268.
- SUND, H. and WEBER, K., *Angew. Chem.*, **78**, (1966) 217.
- SVENSSON, H., *Arkiv Kemi Min. Geol.*, **22A**, (1946) 1.
- SWAISGOOD, H. E., BRUNNER, J. R. and LILLEVIK, H. A., *Biochemistry* **3**, (1964) 1616.
- TANFORD, C., *Physical Chemistry of Macromolecules*, John Wiley & Sons, Inc., New York (1967).
- THOMPSON, T. E. and MACKERNAN, W. M., *Biochem. J.*, **81**, (1961) 12.
- TIMASHEFF, S. N. and TOWNEND, R., *J. Am. Chem. Soc.*, **83**, (1961) 470.
- TOWNEND, R. and TIMASHEFF, S. N., *J. Am. Chem. Soc.*, **82**, (1960) 3168.
- TOWNEND, R., WINTERBOTTOM, R. J. and TIMASHEFF, S. N., *J. Am. Chem. Soc.*, **82**, (1960A) 3161.
- TOWNEND, R., WEINBERGER, L. and TIMASHEFF, S. N., *J. Am. Chem. Soc.*, **82**, (1960B) 3175.
- WARNER, R. C., *J. Am. Chem. Soc.*, **66**, (1944) 1725.
- WAUGH, D. F., *Adv. Prot. Chem.*, **9**, (1954) 325.
- WAUGH, D. F. and VON HIPPEL, P. H., *J. Am. Chem. Soc.*, **78**, (1956) 4576.
- WAUGH, D. F., in *Milk Proteins* (MACKENZIE, H. A.), Acad. Press, New York, Vol. 2, (1971) 3.
- WIEDEMANN, E., *Hev. Chim. Acta*, **30**, (1947) 168.
- WINZOR, D. J. and SCHERAGA, H. A., *Biochemistry* **2**, (1963) 1263.
- ZIMMERMAN, J. K. and ACKERS, G. K., *J. Biol. Chem.*, **246**, (1971) 7289.
- ZIMMERMAN, J. K., COX, D. J. and ACKERS, G. K., *J. Biol. Chem.*, **246**, (1971) 4242.

CURRICULUM VITAE

Herman Nijhuis is te Gennep geboren; na de H.B.S. in Gouda te hebben doorlopen is hij zijn studie aan de Universiteit van Amsterdam begonnen. Na het afleggen van het doctoraal examen, waarvoor hij organische scheikunde als hoofdvak en kristallografie als bijvak heeft gekozen, is hij dit proefschrift gaan voorbereiden aan de Landbouwhogeschool te Wageningen. Gedurende deze periode is hij op het Nederlands Instituut voor Zuivelonderzoek te Ede als gastmedewerker gestageerd geweest. Na het voltooien van dit proefschrift is hij leraar in de scheikunde geworden aan het Dr. Mollercollege te Waalwijk.